

Simplified Information Geometry Approach for Massive MIMO-OFDM Channel Estimation - Part II: Convergence Analysis

Jiyuan Yang, *Student Member, IEEE*, Yan Chen, Mingrui Fan, Xiqi Gao, *Fellow, IEEE*, Xiang-Gen Xia, *Fellow, IEEE*, and Dirk Slock, *Fellow, IEEE*

Abstract—In Part II of this two-part paper, we prove the convergence of the simplified information geometry approach (SIGA) proposed in Part I. For a general Bayesian inference problem, we first show that the iteration of the common second-order natural parameter (SONP) is separated from that of the common first-order natural parameter (FONP). Hence, the convergence of the common SONP can be checked independently. We show that with the initialization satisfying a specific but large range, the common SONP is convergent regardless of the value of the damping factor. For the common FONP, we establish a sufficient condition of its convergence and prove that the convergence of the common FONP relies on the spectral radius of a particular matrix related to the damping factor. We give the range of the damping factor that guarantees the convergence in the worst case. Further, we determine the range of the damping factor for massive MIMO-OFDM channel estimation by using the specific properties of the measurement matrices. Simulation results are provided to confirm the theoretical results.

Index Terms—Convergence, Bayesian inference, information geometry, damping factor.

I. INTRODUCTION

Numerous problems in signal processing eventually come to the issue of computing marginal probability density functions (PDF) from a high dimensional joint PDF. In general, the calculation of direct marginalization could be unaffordable since operations such as matrix inversion could be involved. In the past decades, many works have been devoted to providing an efficient way to compute the (approximate) marginal PDFs under various cases. Among them, Bayesian inference approaches, e.g., message passing, Bethe free energy and etc, have attracted much interest due to their reliable performance and low computational complexities [1]–[9]. Furthermore, besides the two advantages mentioned above, some of them possess favorable results in theory. [5] proposes the Gaussian belief propagation (BP) and shows that Gaussian BP is able to compute true marginal mean. In [6], the powerful approximate message passing (AMP) algorithm is proposed. It has been shown that AMP with Bayes-optimal denoiser can be treated as an exact approximation of loopy BP in the large system limit. When the underlying factor graph is a tree, the expectation propagation (EP) in [8] is convergent and can exactly achieve the Bayes-optimal performance.

Recently, we have introduced the information geometry approach (IGA) to the massive multiple-input multiple-output (MIMO) channel estimation [10]. We also improve the stability of IGA by introducing the damping factor and show that IGA

can obtain accurate a posteriori mean at its fixed point. On the basis of IGA, two new results of IGA are revealed when the constant magnitude pilots are adopted. Based on these new results, we propose a simplified IGA (SIGA) in Part I of this two-part paper [11]. Although proposed for the massive MIMO-OFDM channel estimation, SIGA itself could serve as a generic Bayesian inference method which is suitable for Gaussian priors and constant magnitude measurement matrix. In Part I, it has been shown that at the fixed point, the a posteriori mean obtained by SIGA is asymptotically optimal. Furthermore, SIGA can be implemented efficiently when the measurement matrix has special structure. For example, in massive MIMO channel estimation, the measurement matrix could be constructed by partial DFT matrices, SIGA can be then implemented by fast Fourier transform (FFT), which significantly reduces its computational complexity.

On the other hand, one standard limitation of Bayesian inference approaches is that they only work under the prerequisite that their parameters do converge. However, due to the variety of problems, a unified way of proving convergence of Bayesian inference approaches has not yet been found. Thus, the convergence needs to be proved for individual approaches as well as individual problems. So far, there are only a few methods whose convergence has been relatively well revealed. One sufficient condition named the walk-summability is proposed in [5] for the convergence of Gaussian BP. Then, several extended conditions are proposed by the authors in [12], [13]. In [14], the convergence of orthogonal/vector AMP is proved based on the idea of "convergence in principle". In [15], the convergence of AMP (or, equivalently, generalized AMP) is proved in the special case with Gaussian priors.

Similar to most other Bayesian inference approaches, SIGA suffers from divergence. However, by adding damping factor, its convergence can be significantly improved. This is an interesting observation, since in many iterative Bayesian inference approaches, such as, e.g., AMP, damped updating likewise plays an important role in convergence. In Part II of this two-part paper, we will give a theoretical analysis of the convergence of SIGA. The role of the damping factor in the iteration will also be clarified. We summarize the main contributions as follows:

- We prove the convergence of the common second-order natural parameter (SONP) in SIGA for a general Bayesian inference problem with the measurement matrix of constant magnitude property. We show that the iteration of

the common SONP is separated from that of the common first-order natural parameter (FONP). It is then proved that given the initialization satisfying a specific range, the common SONP is guaranteed to converge regardless of the value of damping factor, where the range of initialization is very large.

- We establish a sufficient condition of the convergence of the common FONP in SIGA. We show that the convergence of the common FONP depends on the spectral radius of the iterating system matrix. On this basis, we further give the range of the damping factor that guarantees the convergence of the common FONP in the worst case.
- We apply the above general theories to the case of massive MIMO-OFDM channel estimation. Specifically, we determine a range of the damping factor that guarantees the convergence of the common FONP in SIGA from the properties of the measurement matrices.

The rest of Part II of this two-part paper is organized as follows. Preliminaries of SIGA are introduced, and its convergence is analyzed in Section II. A range of damping factors that guarantee the convergence of SIGA in massive MIMO-OFDM channel estimation is presented in Section III. Simulation results are provided in Section IV. The conclusion is drawn in Section V.

Notations: The superscripts $(\cdot)^*$, $(\cdot)^T$ and $(\cdot)^H$ denote the conjugate, transpose and conjugate-transpose operator, respectively. We use $\lceil x \rceil$ to denote the largest integer not larger than x . $\mathbf{0}$ denotes zero vector or zero matrix with proper dimension when it fits. $\text{Diag}\{\mathbf{x}\}$ denotes the diagonal matrix with \mathbf{x} along its main diagonal and $\text{diag}\{\mathbf{X}\}$ denotes a vector consisting of the diagonal elements of \mathbf{X} . Define $\mathcal{Z}_N^+ \triangleq \{1, 2, \dots, N\}$ and $\mathcal{Z}_N \triangleq \{0, 1, \dots, N\}$. y_n , $a_{i,j}$ or $[\mathbf{A}]_{i,j}$, and $[\mathbf{A}]_{:,i}$ denote the n -th component of the vector \mathbf{y} , the (i, j) -th component of the matrix \mathbf{A} , and the i -th row of the matrix \mathbf{A} , where the component indices start with 1. $\mathbf{a} < b$ means that each component in vector \mathbf{a} is smaller than the scalar b . $\mathbf{a} < \mathbf{c}$ means that each component in vector \mathbf{a} is smaller than the component in the corresponding position in vector \mathbf{c} . $p_G(\mathbf{h}; \boldsymbol{\mu}, \boldsymbol{\Sigma})$ denotes the PDF of a complex Gaussian distribution $\mathcal{CN}(\boldsymbol{\mu}, \boldsymbol{\Sigma})$ for vector \mathbf{h} of complex random variables.

II. CONVERGENCE OF SIGA

In this section, we first briefly introduce SIGA proposed in [11], more details can be found therein. Then, through re-expressing its iterations, we prove its convergence.

A. SIGA

In Part II, we focus on the following Bayesian inference problem:

$$\mathbf{y} = \mathbf{A}\mathbf{h} + \mathbf{z}, \quad (1)$$

where $\mathbf{y} \in \mathbb{C}^N$ is the observation, $\mathbf{A} \in \mathbb{C}^{N \times M}$ is the deterministic (also known) measurement matrix, \mathbf{A} satisfies constant magnitude property, i.e., $|a_{i,j}| = |a_{m,n}|, \forall i, j, m, n$, $\mathbf{h} \sim \mathcal{CN}(\mathbf{0}, \mathbf{D})$ is the M -dimensional complex Gaussian

random vector to be estimated, its covariance matrix \mathbf{D} is deterministic, known, positive definite and diagonal, $\mathbf{z} \sim \mathcal{CN}(\mathbf{0}, \sigma_z^2 \mathbf{I})$ is the N -dimensional noise vector, and \mathbf{h} and \mathbf{z} are independent with each other. Without loss of generality, assuming that the components of \mathbf{A} have unit magnitude. Our goal is to obtain the *a posteriori* information¹ of \mathbf{h} . Given \mathbf{y} , the *a posteriori* distribution of \mathbf{h} is Gaussian. Thus, the *a posteriori* information of \mathbf{h} is determined by the *a posteriori* mean and the *a posteriori* covariance matrix. We have $p(\mathbf{h}|\mathbf{y}) = p_G(\mathbf{h}; \tilde{\boldsymbol{\mu}}, \tilde{\boldsymbol{\Sigma}})$, where the *a posteriori* mean $\tilde{\boldsymbol{\mu}}$ and covariance matrix $\tilde{\boldsymbol{\Sigma}}$ are given by [16]

$$\tilde{\boldsymbol{\mu}} = \mathbf{D} (\mathbf{A}^H \mathbf{A} \mathbf{D} + \sigma_z^2 \mathbf{I})^{-1} \mathbf{A}^H \mathbf{y}, \quad (2a)$$

$$\tilde{\boldsymbol{\Sigma}} = \left(\mathbf{D}^{-1} + \frac{1}{\sigma_z^2} \mathbf{A}^H \mathbf{A} \right)^{-1}. \quad (2b)$$

In the case of large M and N , it is unaffordable to directly calculate $\tilde{\boldsymbol{\mu}}$ and $\tilde{\boldsymbol{\Sigma}}$ since a large dimensional matrix inversion is involved and the complexity of it is $\mathcal{O}(M^3 + M^2N)$. The aim of SIGA is calculating the approximations of the marginals of the *a posteriori* distribution, i.e., the approximations of $p_i(h_i|\mathbf{y}), i \in \mathcal{Z}_M^+$. Then, the *a posteriori* mean and variance can be obtained. We begin with some essential definitions in SIGA. Given $\mathbf{a}, \mathbf{b} \in \mathbb{C}^M$, define a vector function as $\mathbf{f}(\mathbf{a}, \mathbf{b}) \triangleq [\mathbf{a}^T, \mathbf{b}^T]^T \in \mathbb{C}^{2M}$ and an operator \circ as $\mathbf{a} \circ \mathbf{b} \triangleq \frac{1}{2}(\mathbf{b}^H \mathbf{a} + \mathbf{a}^H \mathbf{b})$. Let $\mathbf{d} = \mathbf{f}(\mathbf{0}, \text{diag}\{-\mathbf{D}^{-1}\}) \in \mathbb{C}^{2M}$ and $\mathbf{t} = \mathbf{f}(\mathbf{h}, \mathbf{h} \circ \mathbf{h}^*) \in \mathbb{C}^{2M}$. Then, $p(\mathbf{h}|\mathbf{y})$ can be expressed as [10], [11]

$$p(\mathbf{h}|\mathbf{y}) = \exp \left\{ \mathbf{d} \circ \mathbf{t} + \sum_{n=1}^N c_n(\mathbf{h}) - \psi_q \right\}, \quad (3a)$$

$$c_n(\mathbf{h}) = \frac{1}{\sigma_z^2} (-\mathbf{h}^H \boldsymbol{\gamma}_n \boldsymbol{\gamma}_n^H \mathbf{h} + y_n \mathbf{h}^H \boldsymbol{\gamma}_n + y_n^* \boldsymbol{\gamma}_n^H \mathbf{h}), \quad (3b)$$

$$\boldsymbol{\gamma}_n = [\mathbf{A}^H]_{:,n} = [a_{n,1}^*, \dots, a_{n,M}^*]^T \in \mathbb{C}^M, \quad (3c)$$

where ψ_q is the normalization factor. In (3a), \mathbf{t} only contains the statistics of single random variables, i.e., h_i and $|h_i|^2, i \in \mathcal{Z}_M^+$, and all the interactions (cross terms), $h_i h_j^*, i \neq j$, are contained in $c_n(\mathbf{h}), n \in \mathcal{Z}_N^+$. SIGA is to approximate each $c_n(\mathbf{h})$ as $\boldsymbol{\xi}_n \circ \mathbf{t}$ in an iterative manner, where $\boldsymbol{\xi}_n \in \mathbb{C}^M$ is referred as to the approximation item. In this way, we have

$$p(\mathbf{h}|\mathbf{y}) \approx p_0(\mathbf{h}; \boldsymbol{\vartheta}_0) = \exp \{ (\mathbf{d} + \boldsymbol{\vartheta}_0) \circ \mathbf{t} - \psi_0 \}, \quad (4)$$

where $\boldsymbol{\vartheta}_0 = \sum_{n=1}^N \boldsymbol{\xi}_n \in \mathbb{C}^{2M}$ and ψ_0 is the normalization factor. The marginals of $p_0(\mathbf{h}; \boldsymbol{\vartheta}_0)$ can be calculated directly since it contains no cross terms between random variables. To obtain $\boldsymbol{\xi}_n, n \in \mathcal{Z}_N^+$, and $\boldsymbol{\vartheta}_0$, SIGA constructs the following three types of manifolds: the original manifold (OM), the objective manifold (OBM) and the auxiliary manifold (AM). The OM is defined as the set of PDFs of M -dimensional complex Gaussian random vectors,

$$\mathcal{M}_{\text{or}} = \{p(\mathbf{h}) = p_G(\mathbf{h}; \boldsymbol{\mu}, \boldsymbol{\Sigma}), \boldsymbol{\mu} \in \mathbb{C}^M, \boldsymbol{\Sigma} \in \mathbb{H}_+^M\}, \quad (5)$$

¹Note that a virtual received signal model ([11, Equation (28)]) is introduced such that the *a posteriori* mean obtained by SIGA can be asymptotically optimal. The proof of convergence of SIGA is the same regardless of which received signal model is used. We consider only the received signal model (1) for the sake of notational simplicity.

where \mathbb{H}_+^M is the set of M dimensional positive definite matrices. The OBM is defined as

$$\mathcal{M}_0 = \{p_0(\mathbf{h}; \boldsymbol{\vartheta}_0) = \exp\{(\mathbf{d} + \boldsymbol{\vartheta}_0) \circ \mathbf{t} - \psi_0(\boldsymbol{\vartheta}_0)\}\}, \quad (6)$$

where $\boldsymbol{\vartheta}_0 = \mathbf{f}(\boldsymbol{\theta}_0, \boldsymbol{\nu}_0)$, $\boldsymbol{\theta}_0 \in \mathbb{C}^M$ and $\boldsymbol{\nu}_0 \in \mathbb{R}^M$ are referred to as the natural parameter (NP), the first-order natural parameter (FONP) and the second-order natural parameter (SONP) of p_0 , respectively, and $\psi_0(\boldsymbol{\vartheta}_0)$ is the free energy (normalization factor). N AMs are defined, where the n -th of them is given by

$$\mathcal{M}_n = \{p_n(\mathbf{h}; \boldsymbol{\vartheta})\}, n \in \mathcal{Z}_N^+, \quad (7a)$$

$$p_n(\mathbf{h}; \boldsymbol{\vartheta}) = \exp\{(\mathbf{d} + \boldsymbol{\vartheta}) \circ \mathbf{t} + c_n(\mathbf{h}) - \psi_n(\boldsymbol{\vartheta})\}, \quad (7b)$$

where $\boldsymbol{\vartheta} = \mathbf{f}(\boldsymbol{\theta}, \boldsymbol{\nu})$, $\boldsymbol{\theta} \in \mathbb{C}^M$ and $\boldsymbol{\nu} \in \mathbb{R}^M$ are referred to as the common NP, the common FONP and the common SONP of p_n , respectively, and $\psi_n(\boldsymbol{\vartheta})$ is the free energy. We call $\boldsymbol{\vartheta}$ the common NP since that all the N AMs share the same $\boldsymbol{\vartheta}$. The OBM and the AMs are submanifolds of the OM since the distributions are all M -dimensional complex Gaussian distributions, but with different constraints [11].

We now introduce the iteration of the SIGA. Mathematically, the iteration of SIGA can be summarized as using the value of $\boldsymbol{\vartheta}$ at the t -th iteration (denoted as $\boldsymbol{\vartheta}(t)$) to compute its value at the $(t+1)$ -th iteration, i.e., $\boldsymbol{\vartheta}(t+1)$, until convergence. After $\boldsymbol{\vartheta}$ is converged, we calculate $\boldsymbol{\vartheta}_0$ as $\boldsymbol{\vartheta}_0 = \frac{N}{N-1}\boldsymbol{\vartheta}$. Then, $p(\mathbf{h}; \boldsymbol{\vartheta}_0)$ in (6) is referred as to the approximation of the product of the marginals of the *a posteriori* distributions, i.e., $\prod_{i=1}^M p_i(h_i|\mathbf{y})$. And the *a posteriori* mean and variance are given by $\boldsymbol{\mu}_0(\boldsymbol{\vartheta}_0)$ and the diagonal of $\boldsymbol{\Sigma}_0(\boldsymbol{\vartheta}_0)$, respectively, where

$$\boldsymbol{\mu}_0(\boldsymbol{\vartheta}_0) = \frac{1}{2}\boldsymbol{\Sigma}_0(\boldsymbol{\vartheta}_0)\boldsymbol{\theta}_0, \quad (8a)$$

$$\boldsymbol{\Sigma}_0(\boldsymbol{\vartheta}_0) = (\mathbf{D}^{-1} - \text{Diag}\{\boldsymbol{\nu}_0\})^{-1}, \quad (8b)$$

and both $\boldsymbol{\mu}_0(\boldsymbol{\vartheta}_0)$ and $\boldsymbol{\Sigma}_0(\boldsymbol{\vartheta}_0)$ are determined by vector $\boldsymbol{\vartheta}_0$. Specifically, given $\boldsymbol{\vartheta}(t) = \mathbf{f}(\boldsymbol{\theta}(t), \boldsymbol{\nu}(t))$ at the t -th iteration, $\boldsymbol{\vartheta}(t+1) = \mathbf{f}(\boldsymbol{\theta}(t+1), \boldsymbol{\nu}(t+1))$ is then calculated as (11) [11], where $0 < d \leq 1$ is the damping factor, and $\boldsymbol{\Lambda}(\boldsymbol{\nu}(t))$ and $\beta(\boldsymbol{\nu}(t))$ are given by

$$\boldsymbol{\Lambda}(\boldsymbol{\nu}(t)) = (\mathbf{D}^{-1} - \text{Diag}\{\boldsymbol{\nu}(t)\})^{-1}, \quad (9a)$$

$$\beta(\boldsymbol{\nu}(t)) = \sigma_z^2 + \text{tr}\{\boldsymbol{\Lambda}(\boldsymbol{\nu}(t))\}. \quad (9b)$$

Briefly, $\boldsymbol{\vartheta}(t+1)$ is obtained by the m -projections of $p_n(\mathbf{h}; \boldsymbol{\vartheta}(t))$, $n \in \mathcal{Z}_N^+$, onto the OBM. The detailed calculation can be found in the Sec. IV of [11]. We summarize the process of the SIGA in Algorithm 1. Comparing to [11, Algorithm 2], we fix the range of $\boldsymbol{\nu}$ in the initialization, i.e.,

$$-\frac{N-1}{\sigma_z^2}\mathbf{1} \leq \boldsymbol{\nu}(0) \leq \mathbf{0}, \quad (10)$$

which will be explained in detail below. We shall see that this new range of $\boldsymbol{\nu}$ will ensure the convergence of SIGA.

Algorithm 1: SIGA

Input: The covariance \mathbf{D} of the a priori distribution $p(\mathbf{h})$, the received signal \mathbf{y} , the noise power σ_z^2 and the maximal iteration number t_{\max} .

Initialization: set $t = 0$, set damping d , where $0 < d \leq 1$, initialize the common NP as

$\boldsymbol{\vartheta}(0) = \mathbf{f}(\boldsymbol{\theta}(0), \boldsymbol{\nu}(0))$ and ensure

$$-\frac{N-1}{\sigma_z^2}\mathbf{1} \leq \boldsymbol{\nu}(0) \leq \mathbf{0};$$

repeat

1. Update $\boldsymbol{\vartheta} = \mathbf{f}(\boldsymbol{\theta}, \boldsymbol{\nu})$ as (11), where $\boldsymbol{\Lambda}(\boldsymbol{\nu}(t))$ and $\beta(\boldsymbol{\nu}(t))$ are given by (9a) and (9b), respectively;

2. $t = t + 1$;

until Convergence or $t > t_{\max}$;

Output: Calculate the NP of $p_0(\mathbf{h}; \boldsymbol{\vartheta}_0)$ as

$\boldsymbol{\vartheta}_0 = \frac{N}{N-1}\boldsymbol{\vartheta}(t)$. The mean and variance of the approximate marginal, $p_i(h_i|\mathbf{y})$, $i \in \mathcal{Z}_M^+$, are given by the i -th component of $\boldsymbol{\mu}_0$ and $\text{diag}\{\boldsymbol{\Sigma}_0\}$, respectively, where $\boldsymbol{\mu}_0$ and $\boldsymbol{\Sigma}_0$ are calculated by (8).

B. Convergence

From Algorithm 1, we can find that to prove the convergence of SIGA, we only need to prove the convergence of $\boldsymbol{\vartheta}(t)$. Given $\boldsymbol{\vartheta}(t) = \mathbf{f}(\boldsymbol{\theta}(t), \boldsymbol{\nu}(t))$ at the t -th time, we re-express $\boldsymbol{\vartheta}(t+1) = \mathbf{f}(\boldsymbol{\theta}(t+1), \boldsymbol{\nu}(t+1))$ in (11) as the follows:

$$\boldsymbol{\nu}(t+1) = \tilde{\mathbf{g}}(\boldsymbol{\nu}(t)) \triangleq d\mathbf{g}(\boldsymbol{\nu}(t)) + (1-d)\boldsymbol{\nu}(t), \quad (12a)$$

$$\mathbf{g}(\boldsymbol{\nu}(t)) = -(N-1)\text{diag}\left\{(\beta(\boldsymbol{\nu}(t))\mathbf{I} - \boldsymbol{\Lambda}(\boldsymbol{\nu}(t)))^{-1}\right\}, \quad (12b)$$

$$\boldsymbol{\theta}(t+1) = \tilde{\mathbf{B}}(\boldsymbol{\nu}(t))\boldsymbol{\theta}(t) + \mathbf{b}(\boldsymbol{\nu}(t)), \quad (13a)$$

$$\tilde{\mathbf{B}}(\boldsymbol{\nu}(t)) \triangleq d\mathbf{B}(\boldsymbol{\nu}(t)) + (1-d)\mathbf{I}, \quad (13b)$$

$$\mathbf{B}(\boldsymbol{\nu}(t)) = \frac{N-1}{\beta(\boldsymbol{\nu}(t))} \left(\mathbf{I} - \frac{1}{\beta(\boldsymbol{\nu}(t))}\boldsymbol{\Lambda}(\boldsymbol{\nu}(t)) \right)^{-1} \times \left(\mathbf{I} - \frac{1}{N}\mathbf{A}^H\mathbf{A} \right) \boldsymbol{\Lambda}(\boldsymbol{\nu}(t)), \quad (13c)$$

$$\mathbf{b}(\boldsymbol{\nu}(t)) = \frac{2d(N-1)}{N\beta(\boldsymbol{\nu}(t))} \left(\mathbf{I} - \frac{1}{\beta(\boldsymbol{\nu}(t))}\boldsymbol{\Lambda}(\boldsymbol{\nu}(t)) \right)^{-1} \mathbf{A}^H\mathbf{y}, \quad (13d)$$

where (12) is the iterating system of $\boldsymbol{\nu}$, (13) is the iterating system of $\boldsymbol{\theta}$, and the derivations are given in Appendix A. All the above matrices that need to be inverted are shown to be invertible at each iteration in Appendix A, which guarantees the iterating systems defined by (12) and (13) are valid, $\tilde{\mathbf{B}}$ and \mathbf{B} are two matrix functions with $\boldsymbol{\nu}(t)$ being the variable, i.e., $\tilde{\mathbf{B}}, \mathbf{B} : \mathbb{R}^M \rightarrow \mathbb{C}^{M \times M}$, and $\mathbf{b}, \tilde{\mathbf{g}}$ and \mathbf{g} are three vector functions with $\boldsymbol{\nu}(t)$ being the variable, i.e., $\mathbf{b} : \mathbb{R}^M \rightarrow \mathbb{C}^M$, and $\tilde{\mathbf{g}}, \mathbf{g} : \mathbb{R}^M \rightarrow \mathbb{R}^M$. Also, we have the following lemma.

Lemma 1. Given a finite initialization $\boldsymbol{\vartheta}(0) = \mathbf{f}(\boldsymbol{\theta}(0), \boldsymbol{\nu}(0))$ with $-\frac{N-1}{\sigma_z^2}\mathbf{1} \leq \boldsymbol{\nu}(0) \leq \mathbf{0}$, then at each iteration, $\boldsymbol{\vartheta}(t) =$

$$\boldsymbol{\theta}(t+1) = \frac{d(N-1)}{N} \left(\mathbf{I} - \frac{1}{\beta(\boldsymbol{\nu}(t))} \boldsymbol{\Lambda}(\boldsymbol{\nu}(t)) \right)^{-1} \left[\frac{1}{\beta(\boldsymbol{\nu}(t))} \mathbf{A}^H (2\mathbf{y} - \mathbf{A}\boldsymbol{\Lambda}(\boldsymbol{\nu}(t))\boldsymbol{\theta}(t)) + N\boldsymbol{\theta}(t) \right] + (1-dN)\boldsymbol{\theta}(t) \quad (11a)$$

$$\boldsymbol{\nu}(t+1) = d(N-1) \text{diag} \left\{ \mathbf{D}^{-1} - \left(\boldsymbol{\Lambda}(\boldsymbol{\nu}(t)) - \frac{1}{\beta(\boldsymbol{\nu}(t))} \boldsymbol{\Lambda}^2(\boldsymbol{\nu}(t)) \right)^{-1} \right\} + (1-dN)\boldsymbol{\nu}(t) \quad (11b)$$

$\mathbf{f}(\boldsymbol{\theta}(t), \boldsymbol{\nu}(t))$ satisfies: $\boldsymbol{\theta}(t)$ and $\boldsymbol{\nu}(t)$ are finite, and $\boldsymbol{\nu}(t) \leq \mathbf{0}$. Specifically, we have $\boldsymbol{\nu}(0) \leq \mathbf{0}$ and $\boldsymbol{\nu}(t) < \mathbf{0}, t \geq 1$.

Proof. See in Appendix A. \square

We refer matrix $\tilde{\mathbf{B}}$ in (13b) as the iterating system matrix of $\boldsymbol{\theta}$, which is determined by the common SONP $\boldsymbol{\nu}$ and the measurement matrix \mathbf{A} at each iteration. Combining (12a) and (13a), we can see that $\boldsymbol{\nu}(t+1)$ only depends on $\boldsymbol{\nu}(t)$ and does not depend on $\boldsymbol{\theta}(t)$, while $\boldsymbol{\theta}(t+1)$ depends on both $\boldsymbol{\theta}(t)$ and $\boldsymbol{\nu}(t)$. This shows that the iterating system of $\boldsymbol{\nu}$ is separated from that of $\boldsymbol{\theta}$, and hence, the convergence of $\boldsymbol{\nu}(t)$ can be checked individually. We then consider the convergence of $\boldsymbol{\nu}(t)$. To this end, we first present the following lemma about the function $\tilde{\mathbf{g}}(\boldsymbol{\nu})$ defined in (12a).

Lemma 2. Given $\boldsymbol{\nu} \leq \mathbf{0}$, $\tilde{\mathbf{g}}(\boldsymbol{\nu})$ satisfies the following two properties.

1. Monotonicity: If $\boldsymbol{\nu} < \boldsymbol{\nu}' \leq \mathbf{0}$, then $\tilde{\mathbf{g}}(\boldsymbol{\nu}) < \tilde{\mathbf{g}}(\boldsymbol{\nu}')$.
2. Scalability: Given a positive constant $0 < \alpha < 1$, we have $\tilde{\mathbf{g}}(\alpha\boldsymbol{\nu}) < \alpha\tilde{\mathbf{g}}(\boldsymbol{\nu})$.

Moreover, if $\tilde{\mathbf{g}}_{\min} \leq \boldsymbol{\nu} \leq \mathbf{0}$ with $\tilde{\mathbf{g}}_{\min} \triangleq -\frac{N-1}{\sigma_z^2} \mathbf{1} \in \mathbb{R}^M$, we have $\tilde{\mathbf{g}}_{\min} < \tilde{\mathbf{g}}(\boldsymbol{\nu}) < \mathbf{0}$.

Proof. See in Appendix B. \square

Based on Lemma 2, we then have the following theorem.

Theorem 1. Given initialization $\boldsymbol{\nu}(0)$ with $\tilde{\mathbf{g}}_{\min} \leq \boldsymbol{\nu}(0) \leq \mathbf{0}$, where $\tilde{\mathbf{g}}_{\min}$ is defined in Lemma 2, the sequence $\boldsymbol{\nu}(t+1) = \tilde{\mathbf{g}}(\boldsymbol{\nu}(t))$ converges to a finite fixed point $\boldsymbol{\nu}^*$, where $\tilde{\mathbf{g}}_{\min} < \boldsymbol{\nu}^* < \mathbf{0}$.

Proof. See in Appendix C. \square

From Theorem 1, we can find that $\boldsymbol{\nu}(t)$ converges to a finite fixed point as long as the initialization satisfies $\tilde{\mathbf{g}}_{\min} \leq \boldsymbol{\nu}(0) \leq \mathbf{0}$, and this range can be quite large. For example, in the simulations of [11], $N = 46080$, and when the noise variance is $\sigma_z^2 = 1$, then we obtain $\tilde{\mathbf{g}}_{\min} = -46079 \times \mathbf{1}$, which is a quite small negative vector. Theorem 1 also shows that the convergence of $\boldsymbol{\nu}(t)$ is not related to the damping factor d . Yet we shall see that the convergence of $\boldsymbol{\theta}(t)$ is related to the choice of the damping factor later. Define

$$\boldsymbol{\Lambda}^* = (\mathbf{D}^{-1} - \text{Diag}\{\boldsymbol{\nu}^*\})^{-1}, \quad (14)$$

$$\beta^* = \sigma_z^2 + \text{tr}\{\boldsymbol{\Lambda}^*\}. \quad (15)$$

From Theorem 1, diagonal matrix $\boldsymbol{\Lambda}^*$ is positive definite and $\beta^* > 0$. From (12a) and $\boldsymbol{\nu}^* = \tilde{\mathbf{g}}(\boldsymbol{\nu}^*)$, we have $\boldsymbol{\nu}^* = \mathbf{g}(\boldsymbol{\nu}^*)$. Then, from the first equation of (42) in Appendix A, we have

$$\frac{N}{N-1} \boldsymbol{\nu}^* = \text{diag} \left\{ \mathbf{D}^{-1} - \left(\boldsymbol{\Lambda}^* - \frac{1}{\beta^*} (\boldsymbol{\Lambda}^*)^2 \right)^{-1} \right\}, \quad (16)$$

which implies that

$$\boldsymbol{\Lambda}^* - \frac{1}{\beta^*} (\boldsymbol{\Lambda}^*)^2 = \left(\mathbf{D}^{-1} - \frac{N}{N-1} \text{Diag}\{\boldsymbol{\nu}^*\} \right)^{-1}. \quad (17)$$

Define

$$\tilde{\mathbf{B}}^* = \tilde{\mathbf{B}}(\boldsymbol{\nu}^*) = d\mathbf{B}^* + (1-d)\mathbf{I}, \quad (18)$$

where $\mathbf{B}^* = \mathbf{B}(\boldsymbol{\nu}^*)$ and $\mathbf{b}^* = \mathbf{b}(\boldsymbol{\nu}^*)$. From the definition, $\tilde{\mathbf{B}}^*$ is determined by the fixed point of the common SONP $\boldsymbol{\nu}^*$ and the measurement matrix \mathbf{A} , which does not vary with iterations. To avoid ambiguity, the iterating system matrix refers in particular to $\tilde{\mathbf{B}}^*$ in the rest of the paper, since the convergence condition for the iterating system of $\boldsymbol{\theta}(t)$ given in the following lemma depends only on the spectral radius of $\tilde{\mathbf{B}}^*$.

Lemma 3. Given a finite initialization $\boldsymbol{\theta}(0) \in \mathbb{C}^{M \times 1}$ and $\boldsymbol{\nu}(0)$ with $-\frac{N-1}{\sigma_z^2} \mathbf{1} \leq \boldsymbol{\nu}(0) \leq \mathbf{0}$. Then, $\boldsymbol{\theta}(t)$ in (13) converges to its fixed point if the spectral radius of $\tilde{\mathbf{B}}^*$ is less than 1, i.e., $\rho(\tilde{\mathbf{B}}^*) < 1$, with $\rho(\tilde{\mathbf{B}}^*) = \max\{|\lambda| : \lambda \text{ is an eigenvalue of } \tilde{\mathbf{B}}^*\}$.

Proof. See in Appendix D. \square

From Lemma 3, we see that when $\boldsymbol{\nu}$ converges and the spectral radius of the iterating system matrix in (18) is less than 1, $\boldsymbol{\theta}$ converges. We next give an analysis of the eigenvalue distribution of $\tilde{\mathbf{B}}^*$ and a theoretical explanation for the improved convergence of $\boldsymbol{\theta}$ under damped updating. We begin with the eigenvalues of \mathbf{B}^* in (18). As mentioned above, when $\boldsymbol{\nu}$ converges to $\boldsymbol{\nu}^*$, from (17) and (18) it is not difficult to obtain

$$\begin{aligned} \mathbf{B}^* &= \frac{N-1}{\beta^*} \left(\mathbf{I} - \frac{1}{\beta^*} \boldsymbol{\Lambda}^* \right)^{-1} \left(\mathbf{I} - \frac{1}{N} \mathbf{A}^H \mathbf{A} \right) \boldsymbol{\Lambda}^* \\ &= \left(\mathbf{I} - \frac{1}{N} \mathbf{D}^{-1} \boldsymbol{\Lambda}^* \right) (N\mathbf{I} - \mathbf{A}^H \mathbf{A}) \left(\frac{1}{\beta^*} \boldsymbol{\Lambda}^* \right). \end{aligned} \quad (19)$$

We can find that \mathbf{B}^* is the product of three matrices. The first matrix of the right hand side of (19) satisfies the following property.

Lemma 4. $\mathbf{I} - \frac{1}{N} \mathbf{D}^{-1} \boldsymbol{\Lambda}^*$ is diagonal with diagonal components all positive and smaller than 1.

Proof. From (14), we can obtain that $\mathbf{0} < \text{diag}\{\mathbf{D}^{-1} \boldsymbol{\Lambda}^*\} < \mathbf{1}$, which implies that the diagonal of $\mathbf{I} - \frac{1}{N} \mathbf{D}^{-1} \boldsymbol{\Lambda}^*$ is positive and smaller than 1. This completes the proof. \square

Since all the three matrices in the product in (19) are Hermitian, we have [17, Exercise below Theorem 5.6.9]

$$\begin{aligned} \rho(\mathbf{B}^*) \\ \leq \rho \left(\mathbf{I} - \frac{1}{N} \mathbf{D}^{-1} \boldsymbol{\Lambda}^* \right) \rho(N\mathbf{I} - \mathbf{A}^H \mathbf{A}) \rho \left(\frac{1}{\beta^*} \boldsymbol{\Lambda}^* \right). \end{aligned} \quad (20)$$

From Lemma 4, we can obtain that

$$\rho\left(\mathbf{I} - \frac{1}{N}\mathbf{D}^{-1}\mathbf{\Lambda}^*\right) < 1. \quad (21)$$

Lemma 5. *The spectral radius of $\mathbf{\Lambda}^*$ satisfies*

$$\rho(\mathbf{\Lambda}^*) < \frac{\beta^*}{N}. \quad (22)$$

Proof. See in Appendix E. \square

We next show some properties of the eigenvalues of \mathbf{B}^* and $\tilde{\mathbf{B}}^*$.

Lemma 6. *Denote the eigenvalues of \mathbf{B}^* as $\lambda_{B,i}, i \in \mathcal{Z}_M^+$. Then, $\{\lambda_{B,i}\}_{i=1}^M$ are all real and*

$$-\frac{\rho(\mathbf{N}\mathbf{I} - \mathbf{A}^H\mathbf{A})}{N} < \lambda_{B,i} < 1. \quad (23)$$

Proof. See in Appendix F. \square

Denote the eigenvalues of the iterating system matrix $\tilde{\mathbf{B}}^*$ in (18) as $\tilde{\lambda}_i, i \in \mathcal{Z}_M^+$. From (18), we have $\tilde{\lambda}_i = d\lambda_{B,i} + 1 - d, i \in \mathcal{Z}_M^+$. We then have the following lemma.

Lemma 7. *The eigenvalues of $\tilde{\mathbf{B}}^*$ are all real and satisfy*

$$1 - d \left(1 + \frac{\rho(\mathbf{N}\mathbf{I} - \mathbf{A}^H\mathbf{A})}{N}\right) < \tilde{\lambda}_i < 1. \quad (24)$$

Proof. This is a direct result from Lemma 6. \square

Combining Lemmas 6 and 7, we have the following theorem.

Theorem 2. *Given a finite initialization $\boldsymbol{\theta}(0) \in \mathbb{C}^{M \times 1}$ and $\boldsymbol{\nu}(0)$ with $-\frac{N-1}{\sigma_z^2}\mathbf{1} \leq \boldsymbol{\nu}(0) \leq \mathbf{0}$. Then, $\boldsymbol{\theta}(t)$ in (13) converges to its fixed point if the damping factor satisfies*

$$d < \frac{2}{1 + \frac{\rho(\mathbf{N}\mathbf{I} - \mathbf{A}^H\mathbf{A})}{N}}. \quad (25)$$

Proof. This is a direct result from Lemmas 3 and 7. \square

From Theorem 2, we can find that SIGA will always converge with a sufficiently small damping factor and the range of d is mainly determined by $\rho(\mathbf{N}\mathbf{I} - \mathbf{A}^H\mathbf{A})$. The spectral radius $\rho(\mathbf{N}\mathbf{I} - \mathbf{A}^H\mathbf{A})$ depends on the measurement matrix \mathbf{A} . We next discuss the range of $\rho(\mathbf{N}\mathbf{I} - \mathbf{A}^H\mathbf{A})$ in the worst case and give the range of damping factor accordingly. The range of $\rho(\mathbf{N}\mathbf{I} - \mathbf{A}^H\mathbf{A})$ and the corresponding range of damping factor in massive MIMO-OFDM channel estimation will be discussed in the next section.

Theorem 3. *The spectral radius of $\mathbf{N}\mathbf{I} - \mathbf{A}^H\mathbf{A}$ satisfies*

$$\rho(\mathbf{N}\mathbf{I} - \mathbf{A}^H\mathbf{A}) \leq NM - N. \quad (26)$$

If $\text{rank}(\mathbf{A}) = 1$, then $\rho(\mathbf{N}\mathbf{I} - \mathbf{A}^H\mathbf{A}) = NM - N$.

Proof. See in Appendix G. \square

Corollary 1. *Given a finite initialization $\boldsymbol{\theta}(0) \in \mathbb{C}^{M \times 1}$ and $\boldsymbol{\nu}(0)$ with $-\frac{N-1}{\sigma_z^2}\mathbf{1} \leq \boldsymbol{\nu}(0) \leq \mathbf{0}$. Then, $\boldsymbol{\theta}(t)$ in (13) converges to its fixed point if the damping factor satisfies $d < \frac{2}{M}$.*

Proof. It is a direct result from Theorems 2 and 3. \square

From Corollary 1, we can find that in the worst case, if $d < \frac{2}{M}$, then SIGA converges.

III. APPLICATION TO MASSIVE MIMO-OFDM CHANNEL ESTIMATION

In this section, we will discuss the range of $\rho(\mathbf{N}\mathbf{I} - \mathbf{A}^H\mathbf{A})$ in massive MIMO-OFDM channel estimation, where the range of d can be expanded. We first consider the case where general pilot sequences with constant magnitude property are adopted. In this case, \mathbf{A} is given in [11, Equation (8)] that is briefly described below. Let us first briefly introduce the system configuration and some notations in [11]. Consider the following uplink massive MIMO-OFDM channel estimation problem: A base station equipped with $N_r = N_{r,v} \times N_{r,h}$ uniform planar array (UPA) serves K single antenna users, where $N_{r,v}$ and $N_{r,h}$ are the numbers of the antennas at each vertical column and horizontal row, respectively. The number of subcarriers and cyclic prefix (CP) length of OFDM modulation are N_c and N_g , respectively. The number of subcarriers used for training is $N_p \leq N_c$. Let $\mathbf{Y} \in \mathbb{C}^{N_r \times N_p}$ and $\mathbf{Z} \in \mathbb{C}^{N_r \times N_p}$ be the space-frequency domain received signal and noise, respectively, then, we have the following received signal model [11]

$$\mathbf{Y} = \sum_{k=1}^K \mathbf{V}\mathbf{H}_k\mathbf{F}^T\mathbf{X}_k + \mathbf{Z}, \quad (27)$$

where \mathbf{V} is defined as

$$\mathbf{V} \triangleq \mathbf{V}_v \otimes \mathbf{V}_h \in \mathbb{C}^{N_r \times F_v F_h N_r},$$

$\mathbf{V}_v \in \mathbb{C}^{N_{r,v} \times F_v N_{r,v}}$ and $\mathbf{V}_h \in \mathbb{C}^{N_{r,h} \times F_h N_{r,h}}$ are partial discrete Fourier transformation (DFT) matrices, i.e.,

$$\mathbf{V}_v = \tilde{\mathbf{I}}_{N_{r,v} \times F_v N_{r,v}} \tilde{\mathbf{V}}_v, \quad \mathbf{V}_h = \tilde{\mathbf{I}}_{N_{r,h} \times F_h N_{r,h}} \tilde{\mathbf{V}}_h,$$

$\tilde{\mathbf{V}}_v$ and $\tilde{\mathbf{V}}_h$ are $F_v N_{r,v}$ and $F_h N_{r,h}$ dimensional DFT matrices, respectively, $\tilde{\mathbf{I}}_{N \times FN}$ is a matrix containing the first N rows of the FN dimensional identity matrix, F_v and F_h are two fine (oversampling) factors, \mathbf{F} is defined as

$$\mathbf{F} \triangleq \tilde{\mathbf{I}}_{N_p \times F_r N_p} \tilde{\mathbf{F}} \tilde{\mathbf{I}}_{F_r N_p \times F_r N_f} \in \mathbb{C}^{N_p \times N_r N_f},$$

$\tilde{\mathbf{F}}$ is the $F_r N_p$ dimensional DFT matrix, $\tilde{\mathbf{I}}_{F_r N_p \times F_r N_f}$ is a matrix containing the first $F_r N_f$ columns of the $F_r N_p$ dimensional identity matrix, i.e., \mathbf{F} is the matrix obtained by $\tilde{\mathbf{F}}$ after row extraction and column extraction,

$$N_f \triangleq \lceil N_p N_g / N_c \rceil,$$

F_r is also a fine factor, $\mathbf{H}_k \in \mathbb{C}^{F_v F_h N_r \times F_r N_f}$ is the beam domain channel matrix of user k , whose components follow the independent complex Gaussian distributions with zero mean and possibly different variances, the diagonal matrix \mathbf{X}_k is the training signal of user k satisfying

$$\mathbf{X}_k^H \mathbf{X}_k = \mathbf{I},$$

and \mathbf{Z} is the noise matrix whose components are independent and identically distributed (i.i.d.) complex Gaussian random variables with zero mean and variance σ_z^2 . For the notational convenience, let

$$\mathbf{F}_d \triangleq \tilde{\mathbf{I}}_{N_p \times F_r N_p} \tilde{\mathbf{F}}, \quad (28)$$

and we have

$$\mathbf{F} = \mathbf{F}_d \tilde{\mathbf{I}}_{F_r N_p \times F_r N_f}. \quad (29)$$

From the definitions, we can obtain that

$$\begin{aligned}\mathbf{V}_v \mathbf{V}_v^H &= F_v N_r N_f \mathbf{I}, \\ \mathbf{V}_h \mathbf{V}_h^H &= F_h N_r N_f \mathbf{I}, \\ \mathbf{F}_d \mathbf{F}_d^H &= F_\tau N_p \mathbf{I}.\end{aligned}$$

Denote the power matrix of beam domain channel as

$$\boldsymbol{\Omega}_k \triangleq \mathbb{E} \{ \mathbf{H}_k \odot \mathbf{H}_k^* \}, k \in \mathcal{Z}_K^+. \quad (30)$$

Due to the channel sparsity, most of the components in $\boldsymbol{\Omega}_k$ are (close to) zero [10], [18]. Then, (27) can be rewritten as

$$\mathbf{Y} = \mathbf{V} \mathbf{H} \mathbf{M} + \mathbf{Z}, \quad (31)$$

where $\mathbf{H} = [\mathbf{H}_1, \mathbf{H}_2, \dots, \mathbf{H}_K] \in \mathbb{C}^{F_v F_h N_r \times K F_\tau N_f}$ and $\mathbf{M} = [\mathbf{X}_1 \mathbf{F}, \mathbf{X}_2 \mathbf{F}, \dots, \mathbf{X}_K \mathbf{F}]^T \in \mathbb{C}^{K F_\tau N_f \times N_p}$. After vectorization, we have

$$\mathbf{y} = \tilde{\mathbf{A}} \tilde{\mathbf{h}} + \mathbf{z}, \quad (32)$$

where $\mathbf{y}, \mathbf{z} \in \mathbb{C}^{N \times 1}$ and $\tilde{\mathbf{h}} \in \mathbb{C}^{\tilde{M} \times 1}$ are the vectorizations of \mathbf{Y} , \mathbf{Z} and \mathbf{H} , respectively, $\tilde{\mathbf{A}} \triangleq \mathbf{M}^T \otimes \mathbf{V} \in \mathbb{C}^{N \times \tilde{M}}$, $N = N_r N_p$, $\tilde{M} = K F_a F_\tau N_r N_f$, and $F_a = F_v F_h$. Since most components in $\tilde{\mathbf{h}}$ are zero, we reduce the dimension of variables by extracting non-zero components. Let

$$\boldsymbol{\omega} \triangleq \text{vec} \{ [\boldsymbol{\Omega}_1, \boldsymbol{\Omega}_2, \dots, \boldsymbol{\Omega}_K] \},$$

and $M \triangleq \|\boldsymbol{\omega}\|_0$ be the number of components in $\tilde{\mathbf{h}}$ with non-zero variance, where $\|\cdot\|_0$ is the ℓ_0 norm. Let the indexes of non-zero components in $\boldsymbol{\omega}$ be $\mathcal{P} \triangleq \{p_1, p_2, \dots, p_M\}$, where $1 \leq p_1 < p_2 < \dots < p_M \leq \tilde{M}$. Define the column extraction matrix as

$$\mathbf{E} \triangleq [\mathbf{e}_{p_1}, \mathbf{e}_{p_2}, \dots, \mathbf{e}_{p_M}] \in \mathbb{C}^{\tilde{M} \times M}, \quad (33)$$

where $\mathbf{e}_i \in \mathbb{C}^{\tilde{M} \times 1}$, $i \in \mathcal{P}$, is the i -th column of the \tilde{M} dimensional identity matrix. (32) can be re-expressed as

$$\mathbf{y} = \mathbf{A} \mathbf{h} + \mathbf{z}, \quad (34)$$

where $\mathbf{A} = \tilde{\mathbf{A}} \mathbf{E} \in \mathbb{C}^{N \times M}$ is the matrix of $\tilde{\mathbf{A}}$ after column extraction, $\mathbf{h} \in \mathbb{C}^{M \times 1} = \mathbf{E}^T \tilde{\mathbf{h}}$ is the vector of $\tilde{\mathbf{h}}$ after variable extraction. In (34), $\mathbf{h} \sim \mathcal{CN}(\mathbf{0}, \mathbf{D})$ with diagonal and positive definite $\mathbf{D} \triangleq \text{Diag} \{ \mathbf{E}^T \boldsymbol{\omega} \}$ and $\mathbf{z} \sim \mathcal{CN}(\mathbf{0}, \sigma_z^2 \mathbf{I})$. We then have the following theorem.

Theorem 4. For matrix \mathbf{A} in (34), we have,

$$\rho(\mathbf{N} \mathbf{I} - \mathbf{A}^H \mathbf{A}) \leq (K F_v F_h F_\tau - 1) N. \quad (35)$$

In this case, if

$$d < \frac{2}{K F_v F_h F_\tau}, \quad (36)$$

then SIGA converges.

Proof. See in Appendix H. \square

For the case with $K = 48$, $M = 29277$, and $F_v = F_h = F_\tau = 2$, when general pilot sequences with constant magnitude property are adopted, $d < 0.0052$ is sufficient to ensure the convergence of SIGA. Note that this range is much larger than the worst case $d < \frac{2}{M} = 6.8 \times 10^{-5}$ in Corollary 1. We finally consider the special case, where the adjustable phase

shift pilots (APSPs) [18], are used. In this case, \mathbf{A} is equal to \mathbf{A}_p of [11, Equation (42)], and we have

$$\mathbf{A} = \tilde{\mathbf{A}}_p \mathbf{E}_p, \quad (37)$$

where

$$\tilde{\mathbf{A}}_p = \mathbf{F}_d \otimes \mathbf{V} \in \mathbb{C}^{N \times F_v F_h F_\tau N},$$

and $\mathbf{E}_p \in \mathbb{C}^{F_v F_h F_\tau N \times M}$ is another column extraction matrix similar with \mathbf{E} in (33), whose detailed definition can be found in [11, above Equation (42)].

Theorem 5. For \mathbf{A} in (37), we have,

$$\rho(\mathbf{N} \mathbf{I} - \mathbf{A}^H \mathbf{A}) \leq (F_v F_h F_\tau - 1) N. \quad (38)$$

In this case, if

$$d < \frac{2}{F_v F_h F_\tau}, \quad (39)$$

then SIGA converges.

Proof. See in Appendix I. \square

For the case with $F_v = F_h = F_\tau = 2$, $d < 0.25$ is sufficient for SIGA to converge.

IV. SIMULATION RESULTS

In this section, we present numerical simulations to illustrate the theoretical results. This section is divided into two parts: the first one focuses on the results for the general case, and the other one focuses on the massive MIMO-OFDM channel estimation.

A. General Case

For the general case, we first generate a matrix $\mathbf{A} \in \mathbb{C}^{N \times M}$ with components drawn from i.i.d. $\mathcal{CN}(0, 1)$ and then normalize its components so that their magnitude is 1. The dimension of \mathbf{A} is set to as $N = 300$ and $M = 150$. In this experiment, the components of \mathbf{h} are drawn from i.i.d. $\mathcal{CN}(0, 1)$, and the noise vector \mathbf{z} is a realization of white complex Gaussian noise. The observation \mathbf{y} is generated according to the received signal model $\mathbf{y} = \mathbf{A} \mathbf{h} + \mathbf{z}$. The variance of the noise \mathbf{z} is chosen to $\sigma_z^2 = 0.15$, and this value could achieve an SNR of 30 dB, where the SNR is defined as $\text{SNR} \triangleq \mathbb{E} \{ \|\mathbf{A} \mathbf{h}\|^2 \} / \mathbb{E} \{ \|\mathbf{z}\|^2 \}$ in this experiment. We focus on the convergence performance of $\boldsymbol{\nu}$ as well as $\boldsymbol{\theta}$ in Part II of this paper. A detailed analysis of the estimation performance of SIGA as well as numerical simulations can be found in [11].

We first present the convergence performance of $\boldsymbol{\nu}$ for different initializations as well as different damping factors. To show the convergence of all components of $\boldsymbol{\nu}$, we use $\|\boldsymbol{\nu}\|_2$ as a metric. The initialization is set to $\boldsymbol{\nu}(0) = \mathbf{0}$, $\boldsymbol{\nu}(0) = \tilde{\mathbf{g}}_{\min} = -\frac{N-1}{\sigma_z^2} \mathbf{1}$, and $\boldsymbol{\nu}(0) = -1000 \times \mathbf{1}$, respectively. The damping factor is set to $d = 1$ and $d = 0.6$, respectively. From Fig. 1, we can find $\|\boldsymbol{\nu}\|_2$ converges to the same fixed point in all settings and the fixed point satisfies $0 < \|\boldsymbol{\nu}^*\|_2 < \|\tilde{\mathbf{g}}_{\min}\|_2$, which is in exact agreement with Theorem 1. Note that the vertical axis of the image uses logarithmic coordinates, which results in $\ln(0) = -\infty$ cannot be drawn on the image. We

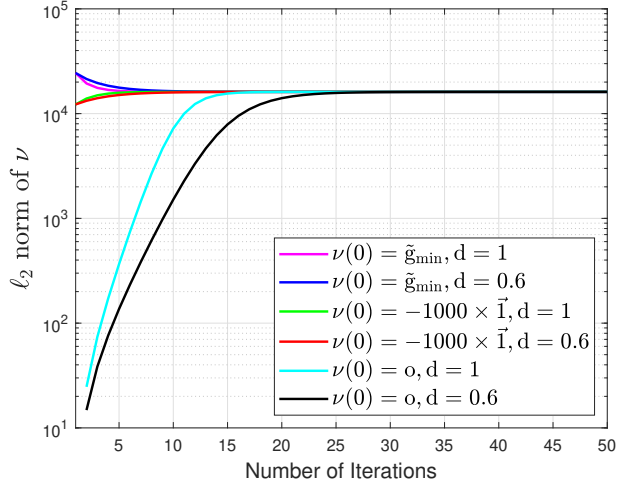


Fig. 1. Convergence of $\|\nu(t)\|$ for different initializations and damping factors in general case.

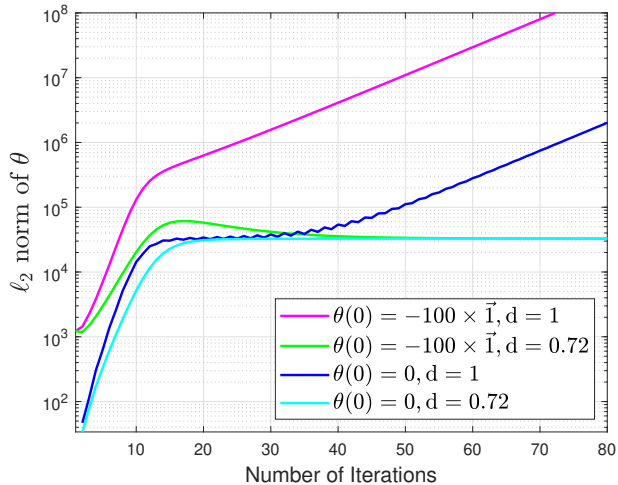


Fig. 2. Convergence and divergence of $\|\theta(t)\|$ for different initializations and damping factors in general case.

also find that the convergence rate of ν slows down with the decrease of the damping factor.

We next show the convergence performance of θ . For \mathbf{A} in this experiment, we calculate $\rho(N\mathbf{I} - \mathbf{A}^H\mathbf{A}) = 528.4643$. According to Theorem 2, $d < 0.7242$ is sufficient for the convergence of θ . We set the damping factor to $d = 1$ and $d = 0.72$, respectively. For simplicity, the initialization of ν is set to $\nu(0) = \mathbf{0}$. The initialization of θ is set to $\theta(0) = \mathbf{0}$ and $\theta(0) = -100 \times \mathbf{1}$, respectively. From Fig. 2, we can find that $\|\theta\|_2$ converges to the same fixed point for all settings except for damping factor $d = 1$ (in this case, $\|\theta\|_2$ diverges). This is exactly consistent with Theorem 2.

B. Massive MIMO Channel Estimation

In this subsection, we focus on the convergence of ν and θ in massive MIMO channel estimation. The system parameter settings as well as the acquisition of \mathbf{h} are detailed as described

in [10], [11]. We summarize the system parameter settings in Table I. Consider two types of pilots: the first is the

TABLE I
PARAMETER SETTINGS

Parameter	Value
Number of BS antenna $N_{r,v} \times N_{r,h}$	8×16
UT number K	48
Center frequency f_c	4.8GHz
Number of training subcarriers N_p	360
Subcarrier spacing Δ_f	15kHz
Number of subcarriers N_c	2048
CP length N_g	144
Fine Factors F_v, F_h, F_τ	2, 2, 2
Mobile velocity of users	3 – 10kmph

general constant magnitude pilot and the other is APSPs. They correspond to the cases described in Theorem 4 and Theorem 5, respectively.

We first consider the general constant magnitude pilot. In this case, the pilots of different users in (27) are generated as $\mathbf{X}_k = \text{diag}\{\mathbf{x}_k\}$, $k \in \mathcal{Z}_K^+$, where the components of \mathbf{x}_k are drawn from i.i.d. $\mathcal{CN}(0, 1)$ and then normalized to the unit magnitude. Then, \mathbf{A} is generated as that in (34). In this experiment, the dimension of \mathbf{A} is calculated as $N = 46080$ and $M = 29277$. The variance of the noise \mathbf{z} is chosen to $\sigma_z^2 = 0.01$, and this value could achieve an SNR of 20 dB, where the SNR is defined as $\text{SNR} \triangleq \frac{1}{\sigma_z^2}$ in this experiment [11]. We then present the convergence performance of ν . The initialization of ν is set to be $\nu(0) = \mathbf{0}$, $\nu(0) = \tilde{\mathbf{g}}_{\min} = -\frac{N-1}{\sigma_z^2} \mathbf{1}$, and $\nu(0) = -\mathbf{1}$, respectively. The damping factor is the same as the previous experiment. From Fig. 3, it can be found that $\|\nu\|_2$ converges to the same fixed point in all settings, where the fixed point satisfies $0 < \|\nu^*\|_2 < \|\tilde{\mathbf{g}}_{\min}\|_2$. This observation is in exact agreement with Theorem 1.

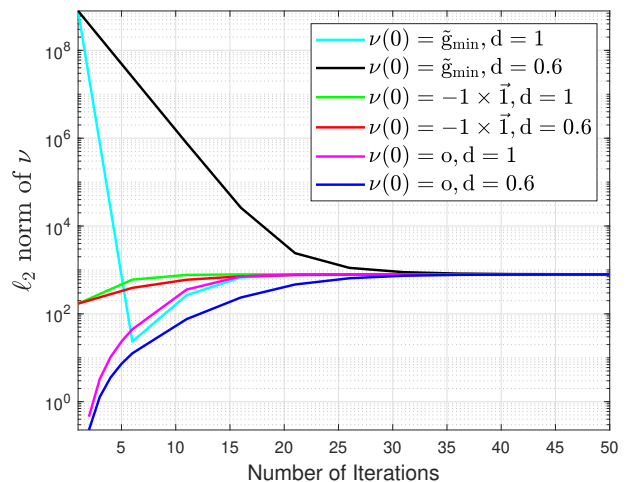


Fig. 3. Convergence of $\|\nu(t)\|$ for different initializations and damping factors for general constant magnitude pilot.

We now show the convergence performance of θ . Due to the large dimension of \mathbf{A} in this experiment, the computational cost of $\rho(N\mathbf{I} - \mathbf{A}^H\mathbf{A})$ is relatively high. We verify the range of damping factor in Theorem 4. The damping factor is set

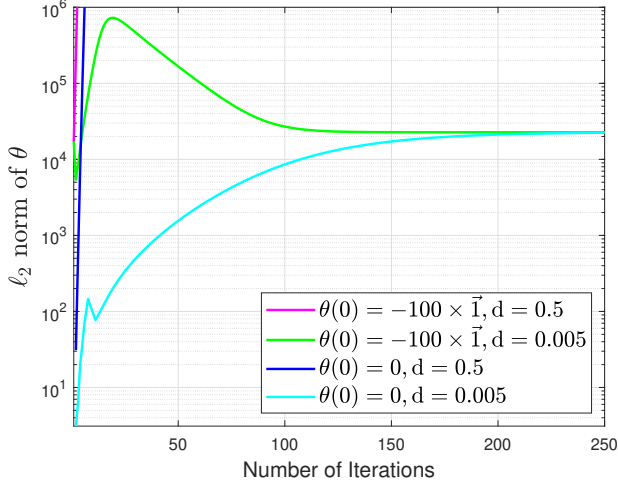


Fig. 4. Convergence and divergence of $\|\theta(t)\|$ for different initializations and damping factors for general constant magnitude pilot.

to be $d = 0.5$ and $d = 0.005$, respectively. From Theorem 4, $d < 0.0052$ is sufficient to ensure the convergence of θ in this experiment. The initialization of ν is set to be $\nu(0) = \mathbf{0}$, and the initialization of θ is set to be $\theta(0) = \mathbf{0}$ and $\theta(0) = -100 \times \mathbf{1}$, respectively. From Fig. 4, it can be found that $\|\theta\|_2$ diverges when $d = 0.5$ and converges to the same fixed point in case of $d = 0.005$. This is consistent with Theorem 4.

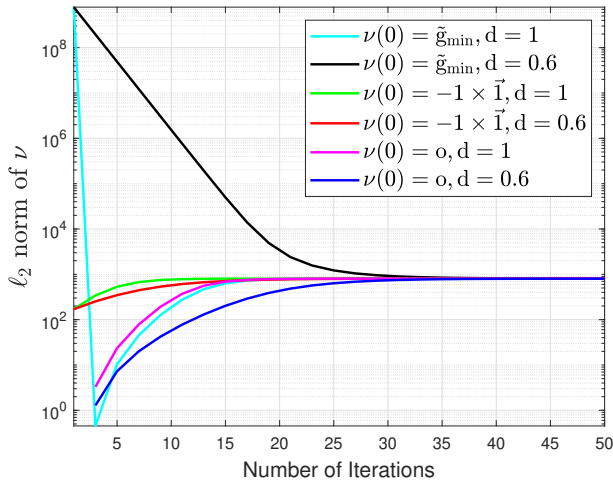


Fig. 5. Convergence of $\|\nu(t)\|$ for different initializations and damping factors for APSPs.

We finally consider the APSPs. The APSP for the user k is set to be $\mathbf{X}_k = \text{Diag}\{\mathbf{r}(n_k)\} \mathbf{P}$, where

$$\mathbf{r}(n_k) = \left[\exp\left\{-j2\pi \frac{n_k N_1}{F_\tau N_p}\right\}, \dots, \exp\left\{-j2\pi \frac{n_k N_2}{F_\tau N_p}\right\} \right]^T \in \mathbb{C}^{N_p}, \quad (40)$$

$n_k \in \{0, 1, \dots, F_\tau N_p - 1\}$ is the phase shift scheduled for the user k , and $\mathbf{P} = \text{Diag}\{\mathbf{p}\}$ is the basic pilot satisfying

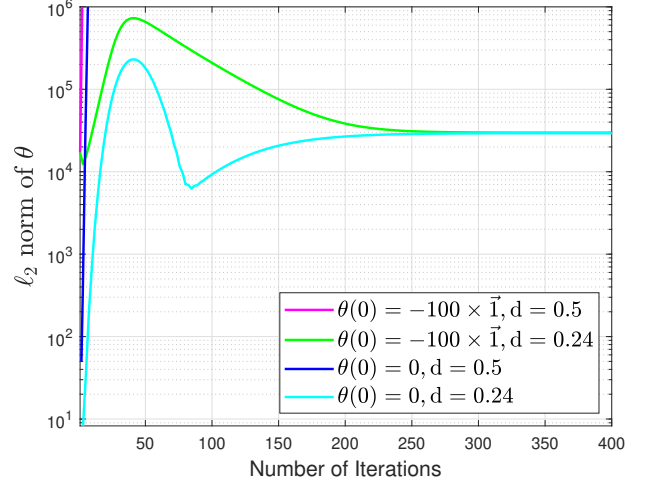


Fig. 6. Convergence and divergence of $\|\theta(t)\|$ for different initializations and damping factors for APSPs.

$\mathbf{P}\mathbf{P}^H = \mathbf{I}$. Given the channel power matrix $\mathbf{\Omega}_k, k \in \mathcal{Z}_K^+$, we can use [18, Algorithm 1] to determine the value of n_k and thus $\mathbf{X}_k, k \in \mathcal{Z}_K^+$. Then, the matrix \mathbf{A} is generated as that in (37) (details can be found in [11]). In this experiment, the dimension of \mathbf{A} is calculated as $N = 46080$ and $M = 29277$. The noise variance σ_z^2 as well as the SNR are the same as in the previous experiment. The convergence performance of ν is plotted in Fig. 5 and similar conclusions can be drawn, where the initialization of ν and the damping factor are the same as in the previous experiment. We then show the convergence performance of θ in Fig. 6, where the damping factor is set to be $d = 0.5$ and $d = 0.24$, respectively, and the initialization of ν and θ is set the same as in the previous experiment. From Theorem 5, $d < 0.25$ is sufficient to ensure the convergence of θ in this experiment. It can be found that $\|\theta\|_2$ diverges when $d = 0.5$ and converges to the same fixed point in case of $d = 0.24$. This is consistent with Theorem 5.

V. CONCLUSION

We have investigated the convergence of SIGA for massive MIMO-OFDM channel estimation. We analyze the convergence of SIGA for a general Bayesian inference problem with the measurement matrix of constant magnitude property, and then apply the general theories to the case of massive MIMO-OFDM channel estimation. Through revisiting its iteration, we find that the iterating system of the common SONP is independent of that of the common FONP. Hence, we can check the convergence of the common SONP separately. It is then proved that given the initialization satisfying a particular and large range, the common SONP is convergent no matter the size of the damping factor. For the convergence of the common FONP, we establish a sufficient condition. More specifically, we find that the convergence of the common FONP depends on the spectral radius of the iterating system matrix $\tilde{\mathbf{B}}^*$. On this basis, we establish condition for the damping factor that guarantees the convergence of $\theta(t)$ in the worst case. Further, we determine the range of the damping factor

for massive MIMO-OFDM channel estimation by using the specific properties of the measurement matrices. Simulation results confirm the theoretical results.

APPENDIX A CALCULATION OF (12)

We first show that $\boldsymbol{\nu}(t+1)$ in (11b) can be re-expressed as that in (12a). From (11b), (41) on the next page is direct. Thus, $\mathbf{g}(\boldsymbol{\nu}(t))$ can be expressed as (42) on the next page, where (a) comes from that (9a). We then show that when $t=0$, the matrices that need to be inverted in (42) are invertible. From (9a) and $\boldsymbol{\nu}(0) \leq \mathbf{0}$, we can obtain that $\boldsymbol{\Lambda}(\boldsymbol{\nu}(0))$ is positive definite and hence invertible. From (9b), we have

$$\beta(\boldsymbol{\nu}(0)) > [\boldsymbol{\Lambda}(\boldsymbol{\nu}(0))]_{i,i} > 0, i \in \mathcal{Z}_M^+.$$

This implies that

$$\beta(\boldsymbol{\nu}(0)) \mathbf{I} - \boldsymbol{\Lambda}(\boldsymbol{\nu}(0))$$

is positive definite and hence invertible. Moreover, combining (41) and (42), we have $\mathbf{g}(\boldsymbol{\nu}(0)) < \mathbf{0}$, and

$$\boldsymbol{\nu}(1) = d\mathbf{g}(\boldsymbol{\nu}(0)) + (1-d)\boldsymbol{\nu}(0) < \mathbf{0}$$

is finite. Following by that, assuming that at the t -th iteration, where $t \geq 1$, we have $\boldsymbol{\nu}(t) < \mathbf{0}$ is finite, $\boldsymbol{\Lambda}(\boldsymbol{\nu}(t))$ and

$$\beta(\boldsymbol{\nu}(t)) \mathbf{I} - \boldsymbol{\Lambda}(\boldsymbol{\nu}(t))$$

are positive definite and invertible. In the same way, it can be readily checked that $\boldsymbol{\nu}(t+1) < \mathbf{0}$ is finite. Hence, we have $\boldsymbol{\Lambda}(\boldsymbol{\nu}(t+1))$ and

$$\beta(\boldsymbol{\nu}(t+1)) \mathbf{I} - \boldsymbol{\Lambda}(\boldsymbol{\nu}(t+1))$$

are positive definite and invertible. By induction, we have shown that when $t \geq 1$, we have $\boldsymbol{\nu}(t) < \mathbf{0}$ is finite, and for $t \geq 0$, $\boldsymbol{\Lambda}(\boldsymbol{\nu}(t))$ and

$$\beta(\boldsymbol{\nu}(t)) \mathbf{I} - \boldsymbol{\Lambda}(\boldsymbol{\nu}(t))$$

are positive definite and invertible.

We now show that $\boldsymbol{\theta}(t+1)$ in (11a) can be re-expressed as that in (13a). From (11a), we can obtain (44), where we omit some of the counter t at the right hand side of the equation for the notational convenience, and

$$\mathbf{T}(\boldsymbol{\nu}) = \left(\mathbf{I} - \frac{1}{\beta(\boldsymbol{\nu})} \boldsymbol{\Lambda}(\boldsymbol{\nu}) \right)^{-1}, \quad (43)$$

where the matrix invertibility comes from (9) directly. Thus, we can obtain

$$\begin{aligned} \mathbf{B}(\boldsymbol{\nu}) & \quad (45) \\ &= \frac{(N-1)}{N} \mathbf{T}(\boldsymbol{\nu}) \left(N\mathbf{I} - \frac{1}{\beta(\boldsymbol{\nu})} \mathbf{A}^H \mathbf{A} \boldsymbol{\Lambda}(\boldsymbol{\nu}) \right) - (N-1) \mathbf{I} \\ &= (N-1) \left[\frac{\mathbf{T}(\boldsymbol{\nu})}{N} \left(N\mathbf{I} - \frac{\mathbf{A}^H \mathbf{A} \boldsymbol{\Lambda}(\boldsymbol{\nu})}{\beta(\boldsymbol{\nu})} \right) - \mathbf{T}(\boldsymbol{\nu}) \mathbf{T}^{-1}(\boldsymbol{\nu}) \right] \\ &= \frac{(N-1)}{\beta(\boldsymbol{\nu})} \mathbf{T}(\boldsymbol{\nu}) \left(\mathbf{I} - \frac{1}{N} \mathbf{A}^H \mathbf{A} \right) \boldsymbol{\Lambda}(\boldsymbol{\nu}). \end{aligned}$$

Also, it is not difficult to show that given a finite $\boldsymbol{\theta}(0)$, $\boldsymbol{\theta}(t)$ is finite at each iteration. This completes the proof.

APPENDIX B PROOF OF LEMMA 2

From Appendix A, it can be checked that given $\boldsymbol{\nu} \leq \mathbf{0}$, $\tilde{\mathbf{g}}(\boldsymbol{\nu})$ and $\mathbf{g}(\boldsymbol{\nu})$ are well defined. Denote $g_i(\boldsymbol{\nu})$, ν_i , d_i and $\lambda_i(\boldsymbol{\nu})$ as the i -th components of $\mathbf{g}(\boldsymbol{\nu})$, $\boldsymbol{\nu}$, the diagonals of \mathbf{D} and $\boldsymbol{\Lambda}(\boldsymbol{\nu})$, respectively, where $i \in \mathcal{Z}_M^+$. Due to $\boldsymbol{\nu} \leq \mathbf{0}$, we have

$$\beta(\boldsymbol{\nu}) = \sigma_z^2 + \sum_{i=1}^M \lambda_i(\boldsymbol{\nu}) > 0, \quad (46a)$$

$$\lambda_i(\boldsymbol{\nu}) = \frac{1}{d_i^{-1} - \nu_i} > 0, \quad (46b)$$

$$\begin{aligned} g_i(\boldsymbol{\nu}) &= -\frac{N-1}{\beta(\boldsymbol{\nu}) - \lambda_i(\boldsymbol{\nu})} \\ &= -\frac{N-1}{\sigma_z^2 + \sum_{i' \neq i} \lambda_{i'}(\boldsymbol{\nu})} < 0. \end{aligned} \quad (46c)$$

From (46c) and (12a), the two properties of $\mathbf{g}(\boldsymbol{\nu})$ and $\tilde{\mathbf{g}}(\boldsymbol{\nu})$, i.e., the monotonicity and the scalability, are not difficult to see. We next show its boundedness.

From the definitions, we have

$$\lim_{\nu_1, \nu_2, \dots, \nu_M \rightarrow -\infty} \beta(\boldsymbol{\nu}) = \sigma_z^2. \quad (47a)$$

From the monotonicity of $\mathbf{g}(\boldsymbol{\nu})$, we can obtain

$$\mathbf{g}(\boldsymbol{\nu}) > \lim_{\nu_1, \nu_2, \dots, \nu_M \rightarrow -\infty} \mathbf{g}(\boldsymbol{\nu}) = -\frac{N-1}{\sigma_z^2} \mathbf{1} = \tilde{\mathbf{g}}_{\min}. \quad (48)$$

Thus, $\tilde{\mathbf{g}}_{\min} < \mathbf{g}(\boldsymbol{\nu}) < \mathbf{0}$. Then, $\tilde{\mathbf{g}}_{\min} < \tilde{\mathbf{g}}(\boldsymbol{\nu}) < \mathbf{0}$ directly follows from the definition of $\tilde{\mathbf{g}}(\boldsymbol{\nu}(t))$ in (12a). This completes the proof.

APPENDIX C PROOF OF THEOREM 1

Consider $\boldsymbol{\nu}(1) = \tilde{\mathbf{g}}(\boldsymbol{\nu}(0))$. If $\boldsymbol{\nu}(1) \leq \boldsymbol{\nu}(0)$, by Lemma 2,

$$\boldsymbol{\nu}(2) = \tilde{\mathbf{g}}(\boldsymbol{\nu}(1)) \leq \tilde{\mathbf{g}}(\boldsymbol{\nu}(0)) = \boldsymbol{\nu}(1). \quad (49)$$

Then, the sequence $\boldsymbol{\nu}(t)$ is a decreasing sequence. By Lemma 2, this sequence is also bounded. Thus, it converges to a finite vector $\boldsymbol{\nu}^*$. Also, by Lemma 2, we have the result of Theorem 1. The case of $\boldsymbol{\nu}(1) \geq \boldsymbol{\nu}(0)$ can be similarly proved. This completes the proof.

APPENDIX D PROOF OF LEMMA 3

Define $\boldsymbol{\theta}^*$ as

$$\boldsymbol{\theta}^* \triangleq \left(\mathbf{I} - \tilde{\mathbf{B}}^* \right)^{-1} \mathbf{b}^*. \quad (50)$$

Since $\rho(\tilde{\mathbf{B}}^*) < 1$, 1 is not an eigenvalue of $\tilde{\mathbf{B}}^*$ and $\mathbf{I} - \tilde{\mathbf{B}}^*$ is invertible. Thus, the above $\boldsymbol{\theta}^*$ exists

We next show that $\boldsymbol{\theta}(t)$ converges to $\boldsymbol{\theta}^*$. Since $\rho(\tilde{\mathbf{B}}^*) < 1$, there exists a matrix norm $\|\cdot\|$ such that [17, Lemma 5.6.10]

$$\|\tilde{\mathbf{B}}^*\| < 1. \quad (51)$$

$$\boldsymbol{\nu}(t+1) = d(N-1) \underbrace{\left(\text{diag} \left\{ \mathbf{D}^{-1} - \left(\boldsymbol{\Lambda}(\boldsymbol{\nu}(t)) - \frac{1}{\beta(\boldsymbol{\nu}(t))} \boldsymbol{\Lambda}^2(\boldsymbol{\nu}(t)) \right)^{-1} \right\} - \boldsymbol{\nu}(t) \right)}_{d\mathbf{g}(\boldsymbol{\nu}(t))} + (1-d)\boldsymbol{\nu}(t) \quad (41)$$

$$\begin{aligned} \mathbf{g}(\boldsymbol{\nu}(t)) &= (N-1) \text{diag} \left\{ \mathbf{D}^{-1} - \left(\boldsymbol{\Lambda}(\boldsymbol{\nu}(t)) - \frac{1}{\beta(\boldsymbol{\nu}(t))} \boldsymbol{\Lambda}^2(\boldsymbol{\nu}(t)) \right)^{-1} \right\} - (N-1)\boldsymbol{\nu}(t) \\ &= (N-1) \text{diag} \left\{ \mathbf{D}^{-1} - \text{Diag} \{ \boldsymbol{\nu}(t) \} - \left(\boldsymbol{\Lambda}(\boldsymbol{\nu}(t)) - \frac{1}{\beta(\boldsymbol{\nu}(t))} \boldsymbol{\Lambda}^2(\boldsymbol{\nu}(t)) \right)^{-1} \right\} \\ &\stackrel{(a)}{=} (N-1) \text{diag} \left\{ \boldsymbol{\Lambda}^{-1}(\boldsymbol{\nu}(t)) - \boldsymbol{\Lambda}^{-1}(\boldsymbol{\nu}(t)) \left(\mathbf{I} - \frac{1}{\beta(\boldsymbol{\nu}(t))} \boldsymbol{\Lambda}(\boldsymbol{\nu}(t)) \right)^{-1} \right\} = -(N-1) \text{diag} \left\{ (\beta(\boldsymbol{\nu}(t)) \mathbf{I} - \boldsymbol{\Lambda}(\boldsymbol{\nu}(t)))^{-1} \right\} \end{aligned} \quad (42)$$

$$\begin{aligned} \boldsymbol{\theta}(t+1) &= \frac{d(N-1)}{N} \mathbf{T}(\boldsymbol{\nu}) \left[\frac{1}{\beta(\boldsymbol{\nu})} \mathbf{A}^H(2\mathbf{y}) - \frac{1}{\beta(\boldsymbol{\nu})} \mathbf{A}^H \mathbf{A} \boldsymbol{\Lambda}(\boldsymbol{\nu}) \boldsymbol{\theta}(t) + N\boldsymbol{\theta}(t) \right] + (1-dN)\boldsymbol{\theta}(t) \\ &= \underbrace{\frac{2d(N-1)}{\beta(\boldsymbol{\nu})N} \mathbf{T}(\boldsymbol{\nu}) \mathbf{A}^H \mathbf{y}}_{\mathbf{b}(\boldsymbol{\nu})} + \underbrace{\left[\frac{d(N-1)}{N} \mathbf{T}(\boldsymbol{\nu}) \left(N\mathbf{I} - \frac{1}{\beta(\boldsymbol{\nu})} \mathbf{A}^H \mathbf{A} \boldsymbol{\Lambda}(\boldsymbol{\nu}) \right) \boldsymbol{\theta}(t) - d(N-1)\boldsymbol{\theta}(t) \right]}_{d\mathbf{B}(\boldsymbol{\nu})\boldsymbol{\theta}(t)} + (1-d)\boldsymbol{\theta}(t) \end{aligned} \quad (44)$$

$$\begin{aligned} \varepsilon(t+1) &= \|\boldsymbol{\theta}(t+1) - \boldsymbol{\theta}^*\| = \|\tilde{\mathbf{B}}(\boldsymbol{\nu}(t))\boldsymbol{\theta}(t) - \tilde{\mathbf{B}}^*\boldsymbol{\theta}^* + \mathbf{b}(\boldsymbol{\nu}(t)) - \mathbf{b}^*\| \\ &= \|\tilde{\mathbf{B}}(\boldsymbol{\nu}(t))(\boldsymbol{\theta}(t) - \boldsymbol{\theta}^*) + (\tilde{\mathbf{B}}(\boldsymbol{\nu}(t)) - \tilde{\mathbf{B}}^*)\boldsymbol{\theta}^* + \mathbf{b}(\boldsymbol{\nu}(t)) - \mathbf{b}^*\| \\ &\leq \|\tilde{\mathbf{B}}(\boldsymbol{\nu}(t))(\boldsymbol{\theta}(t) - \boldsymbol{\theta}^*)\| + \|(\tilde{\mathbf{B}}(\boldsymbol{\nu}(t)) - \tilde{\mathbf{B}}^*)\boldsymbol{\theta}^* + \mathbf{b}(\boldsymbol{\nu}(t)) - \mathbf{b}^*\| \\ &\leq \|\tilde{\mathbf{B}}(\boldsymbol{\nu}(t))\|\varepsilon(t) + \|(\tilde{\mathbf{B}}(\boldsymbol{\nu}(t)) - \tilde{\mathbf{B}}^*)\boldsymbol{\theta}^* + \mathbf{b}(\boldsymbol{\nu}(t)) - \mathbf{b}^*\| \end{aligned} \quad (53)$$

Then, let $\|\cdot\|$ be the vector norm that induces the matrix norm $\|\cdot\|$ [17, Definition 5.6.1]. Define the error between $\boldsymbol{\theta}(t)$ and $\boldsymbol{\theta}^*$ as

$$\varepsilon(t) \triangleq \|\boldsymbol{\theta}(t) - \boldsymbol{\theta}^*\|. \quad (52)$$

Then, we can obtain (53) on the next page. Define a sequence $c(t)$ as

$$c(t) \triangleq \|(\tilde{\mathbf{B}}(\boldsymbol{\nu}(t)) - \tilde{\mathbf{B}}^*)\boldsymbol{\theta}_0^* + \mathbf{b}(\boldsymbol{\nu}(t)) - \mathbf{b}^*\|. \quad (54)$$

Since $\boldsymbol{\nu}$ converges to $\boldsymbol{\nu}^*$, we have

$$\lim_{t \rightarrow \infty} \tilde{\mathbf{B}}(\boldsymbol{\nu}(t)) = \tilde{\mathbf{B}}^*, \quad \lim_{t \rightarrow \infty} \mathbf{b}(\boldsymbol{\nu}(t)) = \mathbf{b}^*,$$

and thus,

$$\lim_{t \rightarrow \infty} c(t) = 0, \quad (55)$$

$$\lim_{t \rightarrow \infty} \|\tilde{\mathbf{B}}(\boldsymbol{\nu}(t))\| = \|\tilde{\mathbf{B}}^*\| < 1. \quad (56)$$

Let

$$\delta_1 \triangleq \frac{1 - \|\tilde{\mathbf{B}}^*\|}{2} > 0, \quad (57)$$

$$\delta_2 \triangleq \|\tilde{\mathbf{B}}^*\| + \delta_1 < 1. \quad (58)$$

To show

$$\lim_{t \rightarrow \infty} \varepsilon(t) = 0,$$

we only need to show that $\forall \epsilon > 0, \exists t_0$, when $t > t_0$, we have

$$\varepsilon(t) < \epsilon.$$

From (55) and (56), we can obtain that $\exists t_1 > 0$, when $t > t_1$, we have

$$c(t) < \frac{\epsilon(1 - \delta_2)}{2},$$

$$\|\tilde{\mathbf{B}}(\boldsymbol{\nu}(t))\| \leq \delta_2.$$

Then, for $t \geq t_1$, we have

$$\varepsilon(t+1) \leq \delta_2 \varepsilon(t) + \frac{\epsilon(1 - \delta_2)}{2},$$

and hence for any positive integer Δt ,

$$\varepsilon(t + \Delta t)$$

$$< \delta_2^{\Delta t} \varepsilon(t) + (\delta_2^{\Delta t-1} + \delta_2^{\Delta t-2} + \dots + \delta_2^0) \frac{\epsilon(1 - \delta_2)}{2}$$

$$< \delta_2^{\Delta t} \varepsilon(t) + \frac{\epsilon}{2}.$$

Since $0 < \delta_2 < 1$, we have

$$\lim_{\Delta t \rightarrow \infty} \delta_2^{\Delta t} = 0.$$

Let Δt such that

$$\delta_2^{\Delta t} < \frac{\epsilon}{2\epsilon(t_1)}.$$

Let $t_0 = t_1 + \Delta t$. Then, when $t > t_0$, we have

$$\begin{aligned} \varepsilon(t) &= \varepsilon(t_0 + t - t_0) = \varepsilon(t_1 + \Delta t + t - t_0) \\ &< \delta_2^{\Delta t + t - t_0} \varepsilon(t_1) + \frac{\epsilon}{2} < \delta_2^{\Delta t} \varepsilon(t_1) + \frac{\epsilon}{2} \\ &< \frac{\epsilon}{2\epsilon(t_1)} \varepsilon(t_1) + \frac{\epsilon}{2} = \epsilon. \end{aligned}$$

This proves

$$\lim_{t \rightarrow \infty} \varepsilon(t) = 0.$$

Since all vector norms are equivalent, it implies that $\|\boldsymbol{\theta}(t) - \boldsymbol{\theta}^*\|_2$ with the Euclidean norm also goes to zero as $t \rightarrow \infty$. This completes the proof of Lemma 3.

APPENDIX E PROOF OF LEMMA 5

From (12a), we have

$$\begin{aligned} \boldsymbol{\nu}^* &= \mathbf{g}(\boldsymbol{\nu}^*) \\ &= -(N-1) \text{diag} \left\{ (\beta^* \mathbf{I} - \boldsymbol{\Lambda}^*)^{-1} \right\}. \end{aligned} \quad (59)$$

From the definition of β^* in (15) and $\boldsymbol{\Lambda}^*$ in (14), we can readily show that $\beta^* \mathbf{I} - \boldsymbol{\Lambda}^*$ is invertible. Since we have proven that $\boldsymbol{\nu}^* < \mathbf{0}$ in Theorem 1, from the definition of $\boldsymbol{\Lambda}^*$ in (14), we can obtain

$$\begin{aligned} \boldsymbol{\Lambda}^* &= (\mathbf{D}^{-1} - \text{Diag} \{ \boldsymbol{\nu}^* \})^{-1} \\ &< (-\text{Diag} \{ \boldsymbol{\nu}^* \})^{-1} = \frac{1}{N-1} (\beta^* \mathbf{I} - \boldsymbol{\Lambda}^*). \end{aligned} \quad (60)$$

From the definition, we can obtain $\boldsymbol{\Lambda}^*$ is diagonal positive definite. Let $\lambda_i^* = [\boldsymbol{\Lambda}^*]_{i,i}$, $i \in \mathcal{Z}_M^+$. Hence, λ_i^* is an eigenvalue of $\boldsymbol{\Lambda}^*$ and $\lambda_i^* > 0$, $i \in \mathcal{Z}_M^+$. Then, from (60), we have

$$\lambda_i^* - \frac{\beta^* - \lambda_i^*}{N-1} < 0, i \in \mathcal{Z}_M^+, \quad (61)$$

which implies that $\lambda_i^* < \frac{\beta^*}{N}$, $i \in \mathcal{Z}_M^+$. Hence, we have $\rho(\boldsymbol{\Lambda}^*) < \frac{\beta^*}{N}$. This completes the proof.

APPENDIX F PROOF OF LEMMA 6

We first prove that the eigenvalues of \mathbf{B}^* are all real. Let

$$\begin{aligned} \mathbf{Q} &\triangleq \left(\mathbf{I} - \frac{1}{N} \mathbf{D}^{-1} \boldsymbol{\Lambda}^* \right)^{1/2} \left(\frac{\boldsymbol{\Lambda}^*}{\beta^*} \right)^{1/2} (\mathbf{N}\mathbf{I} - \mathbf{A}^H \mathbf{A}) \\ &\quad \times \left(\mathbf{I} - \frac{1}{N} \mathbf{D}^{-1} \boldsymbol{\Lambda}^* \right)^{1/2} \left(\frac{\boldsymbol{\Lambda}^*}{\beta^*} \right)^{1/2} \\ &= \mathbf{K}^{-1} \mathbf{B}^* \mathbf{K} \sim \mathbf{B}^*, \end{aligned} \quad (62)$$

where \mathbf{K} is the following diagonal positive definite matrix:

$$\mathbf{K} = \left(\frac{\boldsymbol{\Lambda}^*}{\beta^*} \right)^{-1/2} \left(\mathbf{I} - \frac{1}{N} \mathbf{D}^{-1} \boldsymbol{\Lambda}^* \right)^{1/2}. \quad (63)$$

Thus, \mathbf{B}^* and \mathbf{Q} have the same eigenvalues. From the definition, \mathbf{Q} is Hermitian. Therefore, the eigenvalues of \mathbf{Q} and \mathbf{B}^* are all real. Then, from (64) on the next page, we have

$\mathbf{Q}_1, \mathbf{Q}_2$ are Hermitian, and hence [19, 6.70 (a), pp116]

$$\lambda_{max}(\mathbf{Q}) \leq \lambda_{max}(\mathbf{Q}_1) + \lambda_{max}(\mathbf{Q}_2). \quad (65)$$

Then, for \mathbf{Q}_1 , we can readily check that it is positive definite, and thus

$$\lambda_{max}(\mathbf{Q}_1) = \rho(\mathbf{Q}_1) \stackrel{(a)}{\leq} N \rho \left(\mathbf{I} - \frac{1}{N} \mathbf{D}^{-1} \boldsymbol{\Lambda}^* \right) \rho \left(\frac{\boldsymbol{\Lambda}^*}{\beta^*} \right) \stackrel{(b)}{<} 1, \quad (66)$$

where (a) comes from [17, Exercise below Theorem 5.6.9] and (b) comes from (21) and (37). Define \mathbf{K}_1 as

$$\mathbf{K}_1 = \left(\mathbf{I} - \frac{1}{N} \mathbf{D}^{-1} \boldsymbol{\Lambda}^* \right)^{1/2} \left(\frac{\boldsymbol{\Lambda}^*}{\beta^*} \right)^{1/2}. \quad (67)$$

Then, we can obtain that $-\mathbf{Q}_2 = (\mathbf{A} \mathbf{K}_1)^H \mathbf{A} \mathbf{K}_1$. Hence, \mathbf{Q}_2 is negative semidefinite, and we have $\lambda_{max}(\mathbf{Q}_2) \leq 0$. Thus, we have

$$\lambda_{max}(\mathbf{Q}) < 1. \quad (68)$$

Since $\mathbf{B}^* \sim \mathbf{Q}$, we have $\lambda_{max}(\mathbf{B}^*) < 1$. Then, from (20), we have

$$\rho(\mathbf{B}^*) < 1 \times \rho(\mathbf{N}\mathbf{I} - \mathbf{A}^H \mathbf{A}) \times \frac{1}{N} = \frac{\rho(\mathbf{N}\mathbf{I} - \mathbf{A}^H \mathbf{A})}{N}. \quad (69)$$

Thus, we can obtain that

$$-\frac{\rho(\mathbf{N}\mathbf{I} - \mathbf{A}^H \mathbf{A})}{N} < \lambda_{B,i} < 1.$$

This completes the proof.

APPENDIX G PROOF OF THEOREM 3

We first give the range of $\rho(\mathbf{A}^H \mathbf{A})$. From the definition, $\mathbf{A}^H \mathbf{A}$ is positive semidefinite. The eigenvalues $v_1 \leq v_2 \leq \dots \leq v_M$ of $\mathbf{A}^H \mathbf{A}$ are real and nonnegative. Thus, we can obtain $v_M = \rho(\mathbf{A}^H \mathbf{A})$. Then, we have

$$\begin{aligned} \rho(\mathbf{A}^H \mathbf{A}) &= v_M \leq \sum_{m=1}^M v_m = \text{tr} \{ \mathbf{A} \mathbf{A}^H \} \\ &\leq \sum_{m=1}^M v_M = M \rho(\mathbf{A}^H \mathbf{A}). \end{aligned} \quad (70)$$

When $|a_{i,j}| = 1, \forall i, j$, we can obtain

$$\text{tr} \{ \mathbf{A} \mathbf{A}^H \} = \|\mathbf{A}\|_F^2 = NM. \quad (71)$$

Thus, we have $\rho(\mathbf{A}^H \mathbf{A}) \leq NM \leq M \rho(\mathbf{A}^H \mathbf{A})$, which implies that

$$N \leq \rho(\mathbf{A}^H \mathbf{A}) \leq NM. \quad (72)$$

Hence, we have $0 \leq v_1 \leq \dots \leq v_M \leq NM$. The eigenvalues of $\mathbf{N}\mathbf{I} - \mathbf{A}^H \mathbf{A}$ are $v'_m = N - v_m, m \in \mathcal{Z}_M^+$. Thus, we have $N - NM \leq v'_m \leq N$, and $|v'_m| \leq \max\{N, NM - N\}$. Since in this paper $M > 1$, we have $\rho(\mathbf{N}\mathbf{I} - \mathbf{A}^H \mathbf{A}) \leq NM - N$. If $\text{rank}(\mathbf{A}) = 1$, then \mathbf{A} can be decomposed as $\mathbf{A} = \mathbf{a} \mathbf{b}^H$, where $\mathbf{a} \in \mathbb{C}^{N \times 1}$, $\mathbf{b} \in \mathbb{C}^{M \times 1}$, and \mathbf{a} and \mathbf{b} are non-zero. Combining [19, 6.54 (c)], $\mathbf{b} \mathbf{b}^H$ and $\mathbf{b}^H \mathbf{b}$ are positive semidefinite, we can obtain that

$$\rho(\mathbf{A}^H \mathbf{A}) = \rho(\mathbf{b} \mathbf{a}^H \mathbf{a} \mathbf{b}^H) = \mathbf{a}^H \mathbf{a} \rho(\mathbf{b} \mathbf{b}^H) = \mathbf{a}^H \mathbf{a} \rho(\mathbf{b}^H \mathbf{b})$$

$$\mathbf{Q} = \underbrace{N \left(\mathbf{I} - \frac{1}{N} \mathbf{D}^{-1} \boldsymbol{\Lambda}^* \right) \frac{\boldsymbol{\Lambda}^*}{\beta^*}}_{\mathbf{Q}_1} + \underbrace{\left(\mathbf{I} - \frac{1}{N} \mathbf{D}^{-1} \boldsymbol{\Lambda}^* \right)^{1/2} \left(\frac{\boldsymbol{\Lambda}^*}{\beta^*} \right)^{1/2} (-\mathbf{A}^H \mathbf{A}) \left(\mathbf{I} - \frac{1}{N} \mathbf{D}^{-1} \boldsymbol{\Lambda}^* \right)^{1/2} \left(\frac{\boldsymbol{\Lambda}^*}{\beta^*} \right)^{1/2}}_{\mathbf{Q}_2} \quad (64)$$

$$= \text{tr} \{ \mathbf{A}^H \mathbf{A} \} = NM. \quad (73)$$

Then, we have $\rho(\mathbf{N}\mathbf{I} - \mathbf{A}^H \mathbf{A}) = NM - N$. This completes the proof.

APPENDIX H PROOF OF THEOREM 4

From the definition, we have

$$\mathbf{A}^H \mathbf{A} = \mathbf{E}^T \left(\tilde{\mathbf{A}}^H \tilde{\mathbf{A}} \right) \mathbf{E},$$

which implies that $\mathbf{A}^H \mathbf{A}$ is a principal submatrix of $\tilde{\mathbf{A}}^H \tilde{\mathbf{A}}$. Combining [17, Theorem 4.3.28] and the elementary transformation, we have

$$\lambda_{max}(\mathbf{A}^H \mathbf{A}) \leq \lambda_{max}(\tilde{\mathbf{A}}^H \tilde{\mathbf{A}}), \quad (74)$$

which implies that $\rho(\mathbf{A}^H \mathbf{A}) \leq \rho(\tilde{\mathbf{A}}^H \tilde{\mathbf{A}})$. From [19, 6.54 (c), pp 107], we can obtain $\rho(\tilde{\mathbf{A}}^H \tilde{\mathbf{A}}) = \rho(\tilde{\mathbf{A}} \tilde{\mathbf{A}}^H)$. From the definition, we have

$$\begin{aligned} \tilde{\mathbf{A}} \tilde{\mathbf{A}}^H &= (\mathbf{M}^T \otimes \mathbf{V}) (\mathbf{M}^T \otimes \mathbf{V})^H \\ &= (\mathbf{M}^T \mathbf{M}^*) \otimes (\mathbf{V}_v \otimes \mathbf{V}_h) (\mathbf{V}_v^H \otimes \mathbf{V}_h^H) \\ &= F_v F_h N_r \mathbf{K} \otimes \mathbf{I}, \end{aligned} \quad (75)$$

where $\mathbf{K} = \sum_{k=1}^K \mathbf{X}_k \mathbf{F} \mathbf{F}^H \mathbf{X}_k^H$. Since \mathbf{K} is Hermitian, we can decompose \mathbf{K} as $\mathbf{K} = \mathbf{U} \boldsymbol{\Lambda}_K \mathbf{U}^H$, where \mathbf{U} is unitary. Then, we can obtain

$$\mathbf{K} \otimes \mathbf{I} = (\mathbf{U} \otimes \mathbf{I}) (\boldsymbol{\Lambda}_K \otimes \mathbf{I}) (\mathbf{U}^H \otimes \mathbf{I}) = \mathbf{U}' \boldsymbol{\Lambda}'_K (\mathbf{U}')^H, \quad (76)$$

where \mathbf{U}' is unitary and $\boldsymbol{\Lambda}'_K$ is diagonal. Since $\mathbf{K} \otimes \mathbf{I}$ is also Hermitian, we can obtain that

$$\rho(\mathbf{K} \otimes \mathbf{I}) = \rho(\mathbf{K}).$$

Since \mathbf{X}_k is unitary, we also have $\rho(\mathbf{X}_k \mathbf{F} \mathbf{F}^H \mathbf{X}_k^H) = \rho(\mathbf{F} \mathbf{F}^H)$, $\forall k$. Finally, we have

$$\begin{aligned} \rho(\tilde{\mathbf{A}}^H \tilde{\mathbf{A}}) &= \rho(\tilde{\mathbf{A}} \tilde{\mathbf{A}}^H) = F_v F_h N_r \rho(\mathbf{K}) \\ &\stackrel{(a)}{\leq} F_v F_h N_r \sum_{k=1}^K \rho(\mathbf{F} \mathbf{F}^H) = K F_v F_h N_r \rho(\mathbf{F} \mathbf{F}^H), \end{aligned} \quad (77)$$

where (a) comes from [19, 6.70 (a), pp 116] and $\mathbf{X}_k \mathbf{F} \mathbf{F}^H \mathbf{X}_k^H$ is positive semi-definite. Similarly, we can obtain

$$\begin{aligned} \rho(\mathbf{F} \mathbf{F}^H) &= \rho(\mathbf{F}^H \mathbf{F}) = \rho\left(\tilde{\mathbf{I}}_{F_\tau N_p \times F_\tau N_f}^T \mathbf{F}_d^H \mathbf{F}_d \tilde{\mathbf{I}}_{F_\tau N_p \times F_\tau N_f}\right) \\ &\leq \rho(\mathbf{F}_d^H \mathbf{F}_d) = F_\tau N_p, \end{aligned} \quad (78)$$

and hence,

$$\rho(\mathbf{A}^H \mathbf{A}) \leq K F_v F_h F_\tau N_r N_p = K F_v F_h F_\tau N. \quad (79)$$

From a similar process in Appendix G, we can obtain

$$\rho(\mathbf{N}\mathbf{I} - \mathbf{A}^H \mathbf{A}) \leq K F_v F_h F_\tau N - N. \quad (80)$$

Substituting (80) into the right hand side of (25), we have

$$\frac{2}{1 + \frac{\rho(\mathbf{N}\mathbf{I} - \mathbf{A}^H \mathbf{A})}{N}} \geq \frac{2}{K F_v F_h F_\tau}. \quad (81)$$

In this case, if $d < \frac{2}{K F_v F_h F_\tau}$, then SIGA converges. This completes the proof.

APPENDIX I PROOF OF THEOREM 5

From the definitions, it is not difficult to obtain that

$$\rho(\mathbf{A}^H \mathbf{A}) \leq \rho(\tilde{\mathbf{A}}_p^H \tilde{\mathbf{A}}_p) = \rho(\tilde{\mathbf{A}}_p \tilde{\mathbf{A}}_p^H) = F_v F_h F_\tau N. \quad (82)$$

Hence, we can obtain that

$$\rho(\mathbf{N}\mathbf{I} - \mathbf{A}^H \mathbf{A}) \leq (F_v F_h F_\tau - 1) N.$$

Similarly, substituting the above range into the right hand side of (25), we have

$$\frac{2}{1 + \frac{\rho(\mathbf{N}\mathbf{I} - \mathbf{A}^H \mathbf{A})}{N}} \geq \frac{2}{F_v F_h F_\tau}. \quad (83)$$

In this case, if $d < \frac{2}{F_v F_h F_\tau}$, then SIGA converges. This completes the proof.

REFERENCES

- [1] J. Pearl, *Probabilistic Reasoning in Intelligent Systems: Networks of Plausible Inference*. San Mateo, CA: Morgan Kaufmann, 1988.
- [2] M. I. Jordan, Z. Ghahramani, T. S. Jaakkola, and L. K. Saul, "An introduction to variational methods for graphical models," *Machine learning*, vol. 37, pp. 183–233, Nov. 1999.
- [3] J. Winn, C. M. Bishop, and T. Jaakkola, "Variational message passing," *Journal of Machine Learning Research*, vol. 6, no. 4, Apr. 2005.
- [4] J. Yedidia, W. Freeman, and Y. Weiss, "Constructing free-energy approximations and generalized belief propagation algorithms," *IEEE Trans. Inf. Theory*, vol. 51, no. 7, pp. 2282–2312, Jul. 2005.
- [5] D. M. Malioutov, J. K. Johnson, and A. S. Willsky, "Walk-sums and belief propagation in gaussian graphical models," *The Journal of Machine Learning Research*, vol. 7, pp. 2031–2064, 2006.
- [6] D. L. Donoho, A. Maleki, and A. Montanari, "Message passing algorithms for compressed sensing: I. motivation and construction," in *2010 IEEE Information Theory Workshop on Information Theory (ITW 2010, Cairo)*, Jan. 2010, pp. 1–5.
- [7] S. Rangan, "Generalized approximate message passing for estimation with random linear mixing," in *IEEE ISIT, St. Petersburg, Russia, July 31 - August 5, 2011*, pp. 2168–2172.
- [8] T. P. Minka, "Expectation propagation for approximate bayesian inference," *arXiv preprint arXiv:1301.2294*, 2013.
- [9] D. Zhang, X. Song, W. Wang, G. Fettweis, and X. Q. Gao, "Unifying message passing algorithms under the framework of constrained bethe free energy minimization," *IEEE Trans. Wireless Commun.*, vol. 20, no. 7, pp. 4144–4158, Jul. 2021.
- [10] J. Y. Yang, A.-A. Lu, Y. Chen, X. Q. Gao, X.-G. Xia, and D. T. M. Slock, "Channel estimation for massive MIMO: An information geometry approach," *IEEE Trans. Signal Process.*, vol. 70, pp. 4820–4834, Oct. 2022.

- [11] J. Y. Yang, Y. Chen, A.-A. Lu, W. Zhong, X. Q. Gao, X. You, X.-G. Xia, and D. Slock, "Simplified information geometry approach for massive MIMO-OFDM channel estimation - Part I: algorithm and fixed point analysis," *submitted to IEEE Trans. Signal Process.*
- [12] Q. Su and Y.-C. Wu, "Convergence analysis of the variance in Gaussian belief propagation," *IEEE Trans. Signal Process.*, vol. 62, no. 19, pp. 5119–5131, Oct. 2014.
- [13] —, "On convergence conditions of Gaussian belief propagation," *IEEE Trans. Signal Process.*, vol. 63, no. 5, pp. 1144–1155, Mar. 2015.
- [14] K. Takeuchi, "On the convergence of orthogonal/vector amp: Long-memory message-passing strategy," *IEEE Trans. Inf. Theory*, vol. 68, no. 12, pp. 8121–8138, Dec. 2022.
- [15] S. Rangan, P. Schniter, A. K. Fletcher, and S. Sarkar, "On the convergence of approximate message passing with arbitrary matrices," *IEEE Trans. Inf. Theory*, vol. 65, no. 9, pp. 5339–5351, Sep. 2019.
- [16] S. M. Kay, *Fundamentals of Statistical Signal Processing*. Englewood Cliffs, NJ: Prentice-Hall, 1993.
- [17] R. A. Horn and C. R. Johnson, *Matrix Analysis*. New York, NY, USA: Cambridge Univ. press, 2012.
- [18] L. You, X. Q. Gao, A. L. Swindlehurst, and W. Zhong, "Channel acquisition for massive MIMO-OFDM with adjustable phase shift pilots," *IEEE Trans. Signal Process.*, vol. 64, no. 6, pp. 1461–1476, Mar. 2016.
- [19] G. A. Seber, *A Matrix Handbook for Statisticians*. Hoboken, NJ, USA: Wiley, 2008.